Actuator and Sensor Fault Reconstruction Using an LPV Sliding Mode Observer

Halim Alwi,* Christopher Edwards†
University of Leicester, Leicester, LE1 7RH, United Kingdom.
and
Andrés Marcos, ‡
Deimos Space S.L., Madrid, 28760, Spain.

This paper presents a new actuator and sensor fault reconstruction scheme for Linear Parameter Varying (LPV) systems, based on a sliding mode observer. Two separate observer schemes for actuator and sensor fault reconstruction are presented. For the design of the actuator fault reconstruction scheme, the varying input distribution matrix has been factorized into a fixed and varying component. A virtual system comprising the system matrix and the fixed input distribution matrix is used for the design of the observer. The fixed input distribution matrix facilitates a coordinate transformation which defines the observer gains and ensures a stable closed-loop reduced order sliding motion. The 'output error injection signals' from the observer are used for reconstruction. For the sensor fault design, augmenting the LPV system with a filtered version of the faulty measurements allows the problem of sensor fault reconstruction design to be posed as an actuator fault reconstruction problem. Simulation tests based on an LPV and high-fidelity model of a large transport aircraft have been used to demonstrate the proposed actuator and sensor FDI scheme. The simulation results show good reconstruction of the faults for both actuator and sensors.

Nomenclature

6–DOF	= 6 degree of freedom
FDI, FTC	= Fault detection and isolation, fault tolerant control
LTI, LPV	= Linear time invariant, linear parameter varying
cmd	= command signal
mac	= mean aerodynamic chord
q	= pitch rate
V_{tas}	= true air speed
α, θ, γ	= angle of attack, pitch, flight path angle
h_e	= geometric earth position along the z (altitude) axis
$\mathbb{R}$	= field of real numbers
$\mathcal{R}(A)$	= range space of the matrix A
ρ	= LPV parameter

I. Introduction

Fault Detection and Isolation (FDI) is an important part of active Fault Tolerant Control (FTC).[1,2] The FDI scheme is responsible for providing information about the location and time of any faults/failures which have occurred in the system, thus allowing for example, controller reconfigurations. One of the challenges in FDI, especially for aerospace applications, is dealing with changes in the operating conditions. Although there

*Research Associate, Control & Instrumentation Research Group, Engineering Department.
†Professor, Control & Instrumentation Research Group, Engineering Department.
‡Senior control engineer, Advanced Projects Division. AIAA member

are nonlinear model based FDI approaches (see for example[3–5]), most FDI schemes have been developed based on linear time invariant (LTI) system analysis (e.g.[6–8]). It is claimed in,[9] that ad-hoc methods of controller gain scheduling do not guarantee the required level of performance, or even stability, other than at the points of design, plus the design process is tedious and time consuming. The same argument is also true for observer based FDI. Therefore, a natural extension of the LTI based FDI approaches, is to consider LPV system based FDI (see for example[10–14]) to automatically schedule the observers or detection filter gains. This is motivated by the convenience associated with extending the LTI schemes to LPV systems, which guarantee performance and stability over a wide operating envelope, rather than completely redesigning the scheme to suit nonlinear systems. In terms of aircraft applications, recent papers such as[15] have shown a successful LPV detection filter applied to the longitudinal dynamics of a Boeing 747-100/200 aircraft which is based on the LPV extension of the fundamental problem of residual generation for LTI systems. Although there is extensive literature on LPV based controller design (e.g.[9,16–20]), the literature on LPV observer based FDI or LPV fault detection filters, is still limited and only extensively studied during the last decade. The work of[10–12,15,21,22] and most recently[13,14,23] (and the references therein) represent recent notable work in the field of LPV observer based FDI (and LPV fault detection filters).

In the last few decades, there has been a rise of interest in sliding mode techniques for observer based FDI. One of the reasons is its robustness property to so–called 'matched uncertainty'.[24] The initial sliding mode observer–based FDI work used typical residual based FDI ideas (e.g.[25,26]). The idea was to ensure the sliding motion was broken when faults/failures occurred in the system, and a residual was generated. The more recent work by[27,28] represent some of the approaches which have the capability to reconstruct/identify faults. Not only do these design approaches have the ability to detect and isolate the source of the faults/failures, they also provide further information about the faults/failures (e.g. shape and magnitude) which can be useful for controller reconfiguration. This is something advantageous. In terms of FTC, the availability of a fault reconstruction signal means that sensor faults can be corrected before the measurement signals are used by the controller (for example[29,30]), and the severity of an actuator fault (actuator effectiveness) can be estimated, which is beneficial for controller reconfiguration.[27,31,32]

In recent years, Sliding Mode Observer (SMO) based (FDI) schemes which utilize the concept of 'output error injection signals' have been shown to be capable of robust fault reconstruction while maintaining a sliding motion. Originally conceived in,[33] the methods have evolved to include (Linear Matrix Inequality) LMI based design[34] and robustness to uncertainty[35] and recently have been tested on a nonlinear aircraft benchmark problem as shown in.[30] However all of these methods are based on LTI systems or quasi-linear systems[36] subject to uncertainty and are restricted to near trim conditions. Therefore, it is natural to extend these methods to wider operating conditions by applying the ideas to LPV system description. Although there are LPV based sliding mode control schemes (e.g.[37,38]), there is no (as far as the authors are concerned) LPV based sliding mode FDI schemes in the literature.

This paper proposes an extension of the sliding mode fault reconstruction schemes in[33] for LPV systems, considering both actuator and sensor faults. For actuator faults, in order to extend the SMO LTI methods for LPV systems, and to achieve an observer regular form,[33] it is assumed that the input distribution matrix associated with the actuator faults to be monitored, can be factorized into a fixed and varying part. This factorization is novel compared to the typical assumptions that the input distribution matrix is fixed and time invariant (see for example[39,40]). The LPV observer design is based on the 'virtual system' which includes the factorized fixed distribution matrix, and the varying system matrices. The observer design proposed in this paper is based on the standard multi/parameter varying model design in MATLAB[41] which is adapted for observer design. The SMO gains associated with the linear output injection term are parameter varying, while the gain associated with the nonlinear injection is kept constant.

In the case of sensor faults, the design involves re-formulating the sensor fault problem as an actuator fault reconstruction problem. Therefore the observer design for actuator FDI can also be used for sensor FDI under these conditions. The problem re-formulation is achieved by augmenting the original system with the filtered version of the faulty measurements. The augmentation proposed in this paper is different from the one in[35] where the plant is augmented with filtered versions of all the outputs. By augmenting with only the faulty measurements, the size of the augmented system is kept low. This allows smaller order system matrices to be considered in the LMI analysis during the observer design, which is advantageous.

Simulation tests based on an LPV model of a large transport aircraft from the literature are used to demonstrate the proposed scheme. For actuator fault reconstruction, the example shows the factorizations of the input distribution matrix associated with the actuators to be monitored, and the design procedure for

the observer gains. The simulation tests show good results. The proposed observer is also tested on the full nonlinear high fidelity model of the aircraft.[42] The results show successful reconstruction of faults which are close to the actual faults. For the sensor fault reconstruction, the same example is considered. The designed observer has been tested on both the LPV and the non-linear model of the aircraft. The simulation results show good reconstruction of the sensor faults on both systems.

II. Actuator fault reconstruction for LPV systems

II.A. LPV system description

Consider an LPV plant with actuator faults represented by

$$\dot{x}(t) = A(\rho)x(t) + B(\rho)u(t) + D(\rho)f_i(t) \quad (1)$$

$$y(t) = Cx(t) \quad (2)$$

where $A(\rho) \in \mathbb{R}^{n\times n}, B(\rho) \in \mathbb{R}^{n\times m}, D(\rho) \in \mathbb{R}^{n\times q}$ are parameter varying matrices, $C \in \mathbb{R}^{p\times n}$ is a fixed output distribution matrix and $n > p \geq q$. It is assumed that the inputs $u(t)$ and the outputs $y(t)$ are available for the FDI scheme. The unknown signal $f_i(t) : \mathbb{R}^+ \to \mathbb{R}^q$ and represents the effect of the faults. In fault–free conditions $f_i = 0$, but when $f_i \neq 0$ a fault exists in the system. Assume that the varying parameters, $\rho \in \Omega \subset \mathbb{R}^d$, where Ω is a compact set, are available (i.e. measurable) for the observer scheme which will be proposed.

Assume that for a given ρ, the varying matrix $D(\rho)$ can be perfectly factorized into fixed and varying components as

$$D(\rho) = DE(\rho) \quad (3)$$

where $D \in \mathbb{R}^{n\times q}$, and $E(\rho) \in \mathbb{R}^{q\times q}$ is assumed to be invertible. The assumption that $E(\rho)$ is invertible will assist in the reconstruction of the faults, and be discussed later. This perfect factorization is quite common for over actuated systems or systems with redundancy e.g. large civil aircraft.[42,43] An example of this factorization for a large civil aircraft will be shown later in the paper.

Using (3), the system in (1) can be written as

$$\dot{x}(t) = A(\rho)x(t) + B(\rho)u(t) + D\underbrace{E(\rho)f_i(t)}_{f_\nu(t,\rho)} \quad (4)$$

where the function $f_\nu(t,\rho) : \mathbb{R}_+ \times \mathbb{R}^d \to \mathbb{R}^q$ now represents the (unknown) inputs which will be estimated by the observer. The actual fault $f_i(t)$ can be estimated once estimates of $f_\nu(t,\rho)$ are obtained from the observer. Assume that

$$\|f_\nu(t,\rho)\| < r_1(\rho)\|u\| + \varphi(t,y,\rho) \quad (5)$$

where $r_1(\rho)$ and $\varphi : \mathbb{R}_+ \times \mathbb{R}^p \times \mathbb{R}^m \to \mathbb{R}_+$ are known functions.

Note that the fact that D (which results from the factorization in (3)) is a fixed matrix, allows the LTI observer design strategy in[33] to be extended for the LPV system in (1)-(2).

II.B. LPV sliding mode observer

The proposed observer has the structure

$$\dot{\hat{x}}(t) = A(\rho)\hat{x}(t) + B(\rho)u(t) - G_l(\rho)e_y(t) + G_n\nu(t) \quad (6)$$

where $G_l(\rho), G_n \in \mathbb{R}^{n\times p}$ are the observer gain matrices and $\nu(t)$ represents a discontinuous switched component to induce a sliding motion[33] (which will be defined later). The objective is to force the output estimation error

$$e_y(t) = \hat{y}(t) - y(t) \quad (7)$$

to zero in finite time where $\hat{y}(t) = C\hat{e}(t)$. Once the output error is zero, a sliding mode is said to have been attained[24] on the sliding surface

$$\mathcal{S} = \{e \in \mathbb{R}^n : Ce = 0\} \quad (8)$$

where $e(t) = \hat{x}(t) - x(t)$. During sliding, actuator faults can be estimated using the 'equivalent output injection'[24,33,35,44] signals required to maintain sliding. Details will be given in the arguments that follow.

II.C. Error system analysis

From the definition of e, subtracting (6) from (4) yields the error system

$$\dot{e}(t) \quad = \quad A(\rho)e(t) - G_l(\rho)e_y(t) + G_n\nu(t) - Df_\nu(t,\rho) \tag{9}$$

Assumption 1: $\text{rank}(CD) = q$ where C and D are defined in (1) and (3).

Since D is a fixed matrix and CD is full rank, there exists a coordinate transformation[33] $x(t) \mapsto T_o x(t)$ such that the output distribution matrix has the following structure

$$y(t) = \underbrace{\left[\begin{array}{cc} 0 & T \end{array}\right]}_{C} \left[\begin{array}{c} x_1(t) \\ x_2(t) \end{array}\right] \tag{10}$$

and the fault distribution matrix

$$D = \left[\begin{array}{c} 0 \\ \hline D_2 \end{array}\right] = \left[\begin{array}{c} 0 \\ \hline 0 \\ D_o \end{array}\right] \tag{11}$$

where $D_2 \in \mathbb{R}^{p\times q}$ and $D_o \in \mathbb{R}^{q\times q}$ is nonsingular. In this observer regular form, the error system (9) can be written in detail as

$$\left[\begin{array}{c} \dot{e}_1(t) \\ \dot{e}_2(t) \end{array}\right] = \underbrace{\left[\begin{array}{cc} A_{11}(\rho) & A_{12}(\rho) \\ A_{21}(\rho) & A_{22}(\rho) \end{array}\right]}_{A(\rho)} \left[\begin{array}{c} e_1(t) \\ e_2(t) \end{array}\right] - \underbrace{\left[\begin{array}{c} 0 \\ D_2 \end{array}\right]}_{D} f_\nu(t,\rho) - \left[\begin{array}{c} G_{l_1}(\rho) \\ G_{l_2}(\rho) \end{array}\right] e_y(t) + \left[\begin{array}{c} G_{n_1} \\ G_{n_2} \end{array}\right] \nu(t) \tag{12}$$

where $e_1 \in \mathbb{R}^{n-p}$ and $e_2 \in \mathbb{R}^p$. Here the matrices $G_{l_1}(\rho) \in \mathbb{R}^{(n-p)\times p}$, $G_{l_2}(\rho) \in \mathbb{R}^{p\times p}$, $G_{n_1} \in \mathbb{R}^{(n-p)\times p}$ and $G_{n_2} \in \mathbb{R}^{p\times p}$.

II.D. Choice of Observer Gains

Consider a further state transformation

$$\tilde{e}(t) = \left[\begin{array}{c} \tilde{e}_1(t) \\ e_y(t) \end{array}\right] = T_L \left[\begin{array}{c} e_1(t) \\ e_2(t) \end{array}\right] = \left[\begin{array}{c} e_1(t) + Le_y(t) \\ e_y(t) \end{array}\right] \tag{13}$$

where $T_L \in \mathbb{R}^{n\times n}$ is given by

$$T_L = \left[\begin{array}{cc} I & L \\ 0 & T \end{array}\right] \tag{14}$$

and $L \in \mathbb{R}^{(n-p)\times p}$. The matrix L represents the design freedom. In the new coordinates $\tilde{e}$, the output distribution matrix

$$e_y(t) = \underbrace{\left[\begin{array}{cc} 0 & I \end{array}\right]}_{\tilde{C}} \tilde{e}(t) \tag{15}$$

As in,[35] the matrix L is assumed to have the special structure

$$L = \left[\begin{array}{cc} L_1 & 0 \end{array}\right] \tag{16}$$

where $L_1 \in \mathbb{R}^{(n-p)\times(p-q)}$.

In the new coordinates, the gain associated with the nonlinear injection is chosen as

$$\tilde{G}_n = T_L G_n = \left[\begin{array}{c} 0 \\ I_p \end{array}\right] \tag{17}$$

and the error system from (12) can be written in the new coordinates as

$$\begin{bmatrix} \dot{\tilde{e}}_1(t) \\ \dot{e}_y(t) \end{bmatrix} = \underbrace{\begin{bmatrix} \tilde{A}_{11}(\rho) & \tilde{A}_{12}(\rho) \\ \tilde{A}_{21}(\rho) & \tilde{A}_{22}(\rho) \end{bmatrix}}_{\tilde{A}(\rho)=T_L A(\rho) T_L^{-1}} \begin{bmatrix} \tilde{e}_1(t) \\ e_y(t) \end{bmatrix} - \underbrace{\begin{bmatrix} 0 \\ \tilde{D}_2 \end{bmatrix}}_{\tilde{D}=T_L D} f_\nu(t,\rho) + \underbrace{\begin{bmatrix} \tilde{G}_{l_1}(\rho) \\ \tilde{G}_{l_2}(\rho) \end{bmatrix}}_{\tilde{G}_l(\rho)} e_y(t) + \underbrace{\begin{bmatrix} 0 \\ I \end{bmatrix}}_{\tilde{G}_n} \nu(t) \tag{18}$$

where the fact that $LD_2 = 0$ has been used to obtain the above (because of the structures of D and L in (11) and (16)). By definition, $\tilde{D}_2 = TD_2$ and

$$e_y(t) = \tilde{C}\tilde{e}(t) = \begin{bmatrix} 0 & I_p \end{bmatrix} \tilde{e}(t)$$

and

$$\tilde{A}(\rho) = \begin{bmatrix} \tilde{A}_{11}(\rho) & \tilde{A}_{12}(\rho) \\ \tilde{A}_{21}(\rho) & \tilde{A}_{22}(\rho) \end{bmatrix} = \begin{bmatrix} A_{11}(\rho) + LA_{21}(\rho) & A_{12}(\rho)T^{-1} + LA_{22}(\rho)T^{-1} - \tilde{A}_{11}(\rho)LT^{-1} \\ TA_{21}(\rho) & TA_{22}(\rho)T^{-1} - TA_{21}(\rho)LT^{-1} \end{bmatrix} \tag{19}$$

Due to the special structure of L from (16), $A(\rho)$ from (12) can be further partitioned so that

$$A(\rho) = \left[\begin{array}{c|c} A_{11}(\rho) & A_{12}(\rho) \\ \hline \begin{bmatrix} A_{211}(\rho) \\ A_{212}(\rho) \end{bmatrix} & A_{22}(\rho) \end{array}\right] \tag{20}$$

and therefore $\tilde{A}_{11}(\rho)$ can be written as

$$\tilde{A}_{11}(\rho) = A_{11}(\rho) + L_1 A_{211}(\rho) \tag{21}$$

where $A_{211}(\rho) \in \mathbb{R}^{(p-q)\times(n-p)}$ represents the top $(p-q)$ rows of $A_{21}(\rho)$ in (12). Suppose a matrix L_1 can be chosen such that $\tilde{A}_{11}(\rho)$ is quadratically stable i.e. there exists a symmetric positive definite (s.p.d) matrix $P_1 \in \mathbb{R}^{(n-p)\times(n-p)}$ such that

$$\tilde{A}_{11}(\rho)^{\mathrm{T}} P_1 + P_1 \tilde{A}_{11}(\rho) < 0 \tag{22}$$

for all $\rho \in \Omega$. A choice of observer gain $\tilde{G}_l(\rho)$ is then

$$\tilde{G}_l(\rho) = \begin{bmatrix} \tilde{G}_{l_1}(\rho) \\ \tilde{G}_{l_2}(\rho) \end{bmatrix} = \begin{bmatrix} \tilde{A}_{12}(\rho) \\ \tilde{A}_{22}(\rho) - \tilde{A}_{22}^s \end{bmatrix} \tag{23}$$

where $\tilde{A}_{22}^s$ is a chosen (fixed) stable (Hurwitz) matrix. Substituting (23) into (18) yields

$$\begin{bmatrix} \dot{\tilde{e}}_1(t) \\ \dot{e}_y(t) \end{bmatrix} = \begin{bmatrix} \tilde{A}_{11}(\rho) & 0 \\ \tilde{A}_{21}(\rho) & \tilde{A}_{22}^s \end{bmatrix} \begin{bmatrix} \tilde{e}_1(t) \\ e_y(t) \end{bmatrix} - \begin{bmatrix} 0 \\ \tilde{D}_2 \end{bmatrix} f_\nu(t,\rho) + \begin{bmatrix} 0 \\ I \end{bmatrix} \nu(t) \tag{24}$$

The discontinuous output error injection vector $\nu(t)$ is defined by

$$\nu(t) = -\mathcal{K}(t,y,u,\rho)\|\tilde{D}_2\| \frac{P_o e_y}{\|P_o e_y\|} \tag{25}$$

where $P_o \in \mathbb{R}^{p\times p}$ is a Lyapunov Matrix for $\tilde{A}_{22}^s$, and the scalar $\mathcal{K}(t,y,u,\rho)$ is any function chosen so that

$$\mathcal{K}(t,y,u,\rho) > r_1(\rho)\|u\| + \varphi(t,y,\rho) + \gamma_o \tag{26}$$

where γ_o is a positive scalar.
For the analysis that follows, define $Q_1 \in \mathbb{R}^{(n-p)\times(n-p)}$ and $Q_2 \in \mathbb{R}^{p\times p}$ as (s.p.d.) design matrices. Let $P_o \in \mathbb{R}^{p\times p}$ be a s.p.d solution to the Lyapunov equation

$$(\tilde{A}_{22}^s)^{\mathrm{T}} P_o + P_o \tilde{A}_{22}^s = -Q_2 \tag{27}$$

Using P_o from above, define $\tilde{Q} = \tilde{Q}^{\mathrm{T}} \in \mathbb{R}^{(n-p)\times(n-p)}$ such that

$$\tilde{Q} > \tilde{A}_{21}(\rho)^{\mathrm{T}} P_o Q_2^{-1} P_o \tilde{A}_{21}(\rho) + Q_1 \tag{28}$$

for all $\rho \in \Omega$. Such a $\tilde{Q}$ exists because Ω is a compact set by definition.
Let $P_1 \in \mathbb{R}^{(n-p)\times(n-p)}$ be a s.p.d. matrix satisfying

$$\tilde{A}_{11}(\rho)^{\mathrm{T}} P_1 + P_1 \tilde{A}_{11}(\rho) < -\tilde{Q} \tag{29}$$

It will be demonstrated that

$$V(\tilde{e}_1, e_y) := \tilde{e}_1^{\mathrm{T}} P_1 \tilde{e}_1 + e_y^{\mathrm{T}} P_o e_y \tag{30}$$

is a quadratic Lyapunov function[16] for $\tilde{A}(\rho) - \tilde{G}_l(\rho)\tilde{C}$ since $\dot{V}(\tilde{e}_1, e_y) < 0$ for $\tilde{e}_1, e_y \neq 0$, as shown in the following analysis:
Taking the derivative of (30) yields

$$\dot{V}(\tilde{e}_1, e_y) \leq -\tilde{e}_1^{\mathrm{T}} \tilde{Q} \tilde{e}_1 + \tilde{e}_1^{\mathrm{T}} \tilde{A}_{21}^{\mathrm{T}}(\rho) P_o e_y + e_y^{\mathrm{T}} P_o \tilde{A}_{21}(\rho) \tilde{e}_1 - e_y^{\mathrm{T}} Q_2 e_y + 2 e_y^{\mathrm{T}} P_o \nu - 2 e_y^{\mathrm{T}} P_o \tilde{D}_2 f_\nu \tag{31}$$

Using the fact that

$$\underbrace{(e_y - Q_2^{-1} P_o \tilde{A}_{21}(\rho)\tilde{e}_1)^{\mathrm{T}}}_{\bar{e}_y^{\mathrm{T}}} Q_2 \underbrace{(e_y - Q_2^{-1} P_o \tilde{A}_{21}(\rho)\tilde{e}_1)}_{\bar{e}_y} \equiv$$

$$e_y^{\mathrm{T}} Q_2 e_y - \tilde{e}_1^{\mathrm{T}} \tilde{A}_{21}^{\mathrm{T}}(\rho) P_o e_y - e_y^{\mathrm{T}} P_o \tilde{A}_{21}(\rho) \tilde{e}_1 + \tilde{e}_1^{\mathrm{T}} \tilde{A}_{21}^{\mathrm{T}}(\rho) P_o \tilde{A}_{21}(\rho) \tilde{e}_1 \tag{32}$$

and substituting into (31) yields

$$\begin{aligned}
\dot{V}(\tilde{e}_1, e_y) &\leq -\tilde{e}_1^{\mathrm{T}} \tilde{Q} \tilde{e}_1 + \tilde{e}_1^{\mathrm{T}} \tilde{A}_{21}^{\mathrm{T}}(\rho) P_o Q_2^{-1} P_o \tilde{A}_{21}(\rho) \tilde{e}_1 - \bar{e}_y^{\mathrm{T}} Q_2 \bar{e}_y + 2 e_y^{\mathrm{T}} P_o \nu - 2 e_y^{\mathrm{T}} P_o \tilde{D}_2 f_\nu \\
&= -\tilde{e}_1^{\mathrm{T}} \left(\tilde{Q} - \tilde{A}_{21}^{\mathrm{T}}(\rho) P_o Q_2^{-1} P_o \tilde{A}_{21}(\rho) \right) \tilde{e}_1 - \bar{e}_y^{\mathrm{T}} Q_2 \bar{e}_y + 2 e_y^{\mathrm{T}} P_o \nu - 2 e_y^{\mathrm{T}} P_o \tilde{D}_2 f_\nu \\
&\leq -\tilde{e}_1^{\mathrm{T}} Q_1 \tilde{e}_1 - \bar{e}_y^{\mathrm{T}} Q_2 \bar{e}_y + 2 e_y^{\mathrm{T}} P_o \nu - 2 e_y^{\mathrm{T}} P_o \tilde{D}_2 f_\nu \\
&\leq -\tilde{e}_1^{\mathrm{T}} Q_1 \tilde{e}_1 - \bar{e}_y^{\mathrm{T}} Q_2 \bar{e}_y - 2\mathcal{K}(t, y, u, \rho) \|\tilde{D}_2\| \|P_o e_y\| - 2 e_y^{\mathrm{T}} P_o \tilde{D}_2 f_\nu
\end{aligned} \tag{33}$$

Using (5) and (26), equation (33) can be replaced by

$$\begin{aligned}
\dot{V}(\tilde{e}_1, e_y) &\leq -\tilde{e}_1^{\mathrm{T}} Q_1 \tilde{e}_1 - \bar{e}_y^{\mathrm{T}} Q_2 \bar{e}_y - 2\mathcal{K}(t, y, u, \rho) \|\tilde{D}_2\| \|P_o e_y\| + 2\|\tilde{D}_2\| (r_1(\rho)\|u\| + \varphi(y)) \|P_o e_y\| \\
&\leq -\tilde{e}_1^{\mathrm{T}} Q_1 \tilde{e}_1 - \bar{e}_y^{\mathrm{T}} Q_2 \bar{e}_y - 2\gamma_o \|\tilde{D}_2\| \|P_o e_y\| \\
&< 0 \quad \text{for} \quad (\tilde{e}_1, e_y) \neq 0
\end{aligned} \tag{34}$$

It follows the error system (9) is quadratically stable. Furthermore, an ideal sliding motion takes place on $\mathcal{S}$ as shown on the following analysis:

Let $a_{21} = \max_{\rho\in\Omega} \|\tilde{A}_{21}(\rho)\|$. The scalar a_{21} is finite because Ω is a compact set. Then for a given scalar $0 < \eta < \|\tilde{D}_2\|\gamma_0$, let r_o be the largest positive scalar such that

$$\mathcal{V}_{r_o} = \{(\tilde{e}_1, e_y) : V(\tilde{e}_1, e_y) < r_o\} \subseteq \{(\tilde{e}_1, e_y) : \|\tilde{e}_1\| < (\|\tilde{D}_2\|\gamma_o - \eta)/a_{21}\}$$

Because $(\tilde{e}_1, e_y) \to 0$ as $t \to \infty$ it follows from the stability arguments above that there exists a time t_o such that for all $t > t_o$ the set $\mathcal{V}_{r_o}$ is invariant. The idea is to show inside the set $\mathcal{V}_{r_o}$, a sliding motion takes place on $\mathcal{S} = \{(\tilde{e}_1, e_y) : e_y = 0\}$. Define

$$V_s = e_y^{\mathrm{T}} P_o e_y$$

then

$$\dot{V}_s = 2 e_y^{\mathrm{T}} P_o \tilde{A}_{21}(\rho) \tilde{e}_1 - e_y^{\mathrm{T}} Q_2 e_y + 2 e_y^{\mathrm{T}} P_o \nu - 2 e_y^{\mathrm{T}} P_o \tilde{D}_2 f_\nu \tag{35}$$

$$\leq 2 a_{21} \|\tilde{e}_1\| \|P_o e_y\| - e_y^{\mathrm{T}} Q_2 e_y - 2\gamma_o \|\tilde{D}_2\| \|P_o e_y\| \tag{36}$$

Therefore, inside $\mathcal{V}_{r_o}$ the inequality $a_{21}\|\tilde{e}_1\| < \|\tilde{D}_2\|\gamma_o - \eta$ holds and

$$\begin{aligned} \dot{V}_s &\leq 2(\|\tilde{D}_2\|\gamma_o - \eta)\|P_o e_y\| - e_y^{\mathrm{T}} Q_2 e_y - 2\gamma_o\|\tilde{D}_2\|\|P_o e_y\| && (37)\\ &\leq -2\eta\|P_o e_y\| && (38)\end{aligned}$$

Using the fact that

$$\|P_o e_y\|^2 = (P_o^{\frac{1}{2}} e_y)^{\mathrm{T}} P_o (P_o^{\frac{1}{2}} e_y) \geq \lambda_{min}(P_o)\|P_o^{\frac{1}{2}} e_y\|^2 = \lambda_{min}(P_o) V_s$$

equation (38) becomes

$$\dot{V}_s \leq -2\eta\lambda_{min}(P_o)^{\frac{1}{2}}\|P_o^{\frac{1}{2}} e_y\| = -2\eta\lambda_{min}(P_o)^{\frac{1}{2}} V_s^{\frac{1}{2}}$$

and therefore $V_s \to 0$ in finite time – i.e. sliding is achieved.

II.E. LMI design

The design freedom matrix L_1, can be synthesized from an LMI perspective using the single quadratic Lyapunov function approach[16] according to

$$\begin{aligned} (A_{11}(\rho) + L_1 A_{211}(\rho))^{\mathrm{T}} P_1 + P_1 (A_{11}(\rho) + L_1 A_{211}(\rho)) < 0 && (39)\\ P_1 > 0 && (40)\end{aligned}$$

In the example (which will be shown later), the solution for P_1 and the design gain L_1 are obtained as part of the output of the standard MATLAB LMI multi-model state feedback synthesis code 'msfsyn'[41] adapted to tackle an observer problem (i.e. the dual of the standard control problem). In the example, a 'pole placement' design is chosen to place the closed-loop pole inside a pre-specified LMI region.[41,45]

II.F. Fault Reconstructions

It is clear from (24) that the reduced order sliding motion when the system is restricted to the surface $\mathcal{S}$ is given by

$$\dot{\tilde{e}}_1 = \tilde{A}_{11}(\rho)\tilde{e}_1 \tag{41}$$

From (24), it follows that

$$\dot{e}_y(t) = A_{21}(\rho)\tilde{e}_1(t) + A_{22}^s e_y(t) - \tilde{D}_2 f_\nu(t,\rho) + \nu(t) \tag{42}$$

During sliding, $\dot{e}_y(t) = e_y(t) = 0$ and since $\tilde{A}_{11}(\rho)$ is stable, $\tilde{e}_1(t) \to 0$ and (42) becomes

$$\nu(t) = \tilde{D}_2 f_\nu(t,\rho) \tag{43}$$

Therefore the output fault $f_\nu(t,\rho)$ can be reconstructed online using the expression

$$\hat{f}_\nu(t) = \tilde{D}_2^\dagger \nu_{eq}(t) \tag{44}$$

where $\tilde{D}_2^\dagger$ is the pseudo inverse of the matrix $\tilde{D}_2$ and $\nu_{eq}(t)$ is the so-called 'equivalent output injection' signal[33] which is required to maintain a sliding motion.

By assumption $E(\rho)$ is invertible and using (4), the actual actuator fault can be estimated as

$$\hat{f}_i(t) = E(\rho)^{-1}\hat{f}_\nu(t) \tag{45}$$

Using (44), the above can be written as

$$\hat{f}_i(t) = \underbrace{E(\rho)^{-1}}_{varying}\ \underbrace{\tilde{D}_2^\dagger}_{fixed}\ \nu_{eq}(t) \tag{46}$$

In the original coordinates, the observer gains can be written as

$$G_l(\rho) = T_o^{-1} T_L^{-1} \tilde{G}_l(\rho),\ G_n = T_o^{-1} T_L^{-1} \tilde{G}_n \tag{47}$$

III. Sensor fault reconstruction for LPV systems

III.A. LPV system with sensor faults

For the sensor fault reconstruction problem, consider an LPV plant represented by

$$\dot{x}(t) = A(\rho)x(t) + B(\rho)u(t) \tag{48}$$
$$y(t) = Cx(t) + Nf_o(t) \tag{49}$$

where $f_o(t) \in \mathbb{R}^r$ is the (unknown) vector of sensor faults and $N \in \mathbb{R}^{p\times r}$ where $\text{rank}(N) = r$ and $r \leq p$. Here, it will be assumed that some of the sensors are fault-free while some are prone to faults. This is not an unreasonable assumption - some may be inherently less reliable or more vulnerable to external damage. By permutating the order of the outputs, without loss of generality assume that the sensor measurements that define the varying parameters ρ are fault-free. Assume that the plant representation is in a form where the outputs which are prone to faults are in the lower half of the output equations, i.e.

$$y(t) = \left[\begin{array}{c} y_1(t) \\ \hline y_2(t) \end{array}\right] \begin{array}{l} \}\text{fault free} \\ \}\text{prone to fault} \end{array} = \underbrace{\left[\begin{array}{c} C_1 \\ \hline C_2 \end{array}\right]}_{C} x(t) + \underbrace{\left[\begin{array}{c} 0 \\ \hline N_2 \end{array}\right]}_{N} f_o(t) \tag{50}$$

where $C_1 \in \mathbb{R}^{(p-r)\times n}$, $C_2 \in \mathbb{R}^{r\times n}$ and $N_2 \in \mathbb{R}^{r\times r}$. This, in the simplest case, can be obtained simply by permutating the rows of C. Otherwise, the outputs could be multiplied by an orthogonal transformation matrix associated with QR reduction of N.[46]

III.B. Development of an Augmented system

The idea here is to re-formulate the sensor fault reconstruction problem such that the fault reconstruction scheme in Section II can be used to estimate $f_o(t)$. Consider a new state $z_f(t) \in \mathbb{R}^r$ which is the filtered output of $y_2(t)$: specifically

$$\dot{z}_f(t) = -A_f z_f(t) + A_f y_2(t) \tag{51}$$

where $-A_f$ is a stable matrix of dimension $\mathbb{R}^{r\times r}$. Substituting $y_2(t)$ from (50) into (51) yields

$$\dot{z}_f(t) = -A_f z_f(t) + A_f C_2 x(t) + A_f N_2 f_o(t) \tag{52}$$

Next, augment system (48) and (52) to form one of the order $(n + r)$ in the form

$$\underbrace{\left[\begin{array}{c} \dot{x}(t) \\ \dot{z}_f(t) \end{array}\right]}_{\dot{x}_a} = \underbrace{\left[\begin{array}{cc} A(\rho) & 0 \\ A_f C_2 & -A_f \end{array}\right]}_{A_a(\rho)} \underbrace{\left[\begin{array}{c} x(t) \\ z_f(t) \end{array}\right]}_{x_a} + \underbrace{\left[\begin{array}{c} B(\rho) \\ 0 \end{array}\right]}_{B_a(\rho)} u(t) + \underbrace{\left[\begin{array}{c} 0 \\ A_f N_2 \end{array}\right]}_{F_a} f_0(t) \tag{53}$$

Next, replace the system output $y_2(t)$ from (50), with the filtered version in (52), where the new 'output' (of the augmented system) becomes

$$\underbrace{\left[\begin{array}{c} y_1(t) \\ z_f(t) \end{array}\right]}_{y_a} = \underbrace{\left[\begin{array}{cc} C_1 & 0 \\ 0 & I_r \end{array}\right]}_{C_a} \underbrace{\left[\begin{array}{c} x(t) \\ z_f(t) \end{array}\right]}_{x_a} \tag{54}$$

Note that augmenting the system (48) with only the faulty senors (52) is different from the one proposed in[35] where the system is augmented with all the filtered outputs of the plant. Now the output is a combination of the actual and the filtered outputs (which are prone to faults). Also note that system (53) above is in the form of (4). Now an observer can be designed by replacing $(A(\rho), D, C)$ in (9) and (7) with $(A_a(\rho), F_a, C_a)$ in (53) and (54) respectively. Also note that by construction, $\text{rank}(C_a F_a) = r$ where C_a and F_a are defined in (54) and (53).

In order to be able to use the scheme in Section II, another change of coordinates is required such that the augmented system outputs are in the form in (15). To achieve this, consider a coordinate transformation $x_a \mapsto T_a x_a = \hat{x}_a$ where

$$\underbrace{\begin{bmatrix} \hat{x}(t) \\ z_f(t) \end{bmatrix}}_{\hat{x}_a} = \underbrace{\begin{bmatrix} T_s & 0 \\ 0 & I_r \end{bmatrix}}_{T_a} \underbrace{\begin{bmatrix} x_1(t) \\ z_f(t) \end{bmatrix}}_{x_a} = \begin{bmatrix} T_s x(t) \\ z_f(t) \end{bmatrix} \tag{55}$$

and $T_s \in \mathbb{R}^{n\times n}$ is any nonsingular matrix such that $C_1 T_s = \begin{bmatrix} 0 & I_{p-r} \end{bmatrix}$. Then, in the new coordinates, the augmented system output becomes

$$\hat{C}_a = \underbrace{\begin{bmatrix} C_1 & 0 \\ 0 & I_r \end{bmatrix}}_{C_a} \underbrace{\begin{bmatrix} T_s & 0 \\ 0 & I_r \end{bmatrix}}_{T_a^{-1}} = \begin{bmatrix} C_1 T_s^{-1} & 0 \\ 0 & I_r \end{bmatrix} = \begin{bmatrix} \begin{bmatrix} 0 & I_{p-r} \end{bmatrix} & 0 \\ 0 & I_r \end{bmatrix} = \begin{bmatrix} 0 & I_p \end{bmatrix} \tag{56}$$

and the augmented system in (53) becomes

$$\dot{\hat{x}}_a = \hat{A}_a(\rho) x_a(t) + \hat{B}_a(\rho) u(t) + \hat{F}_a f_o(t) \tag{57}$$

where

$$\hat{A}_a(\rho) = \begin{bmatrix} \hat{A}_{11}(\rho) & 0 \\ \hat{A}_{21} & \hat{A}_{22} \end{bmatrix} = \begin{bmatrix} T_s A(\rho) T_s^{-1} & 0 \\ A_f C_2 T_s^{-1} & -A_f \end{bmatrix} \tag{58}$$

$$\hat{B}_a(\rho) = \begin{bmatrix} \hat{B}(\rho) \\ 0 \end{bmatrix} = \begin{bmatrix} T_s B(\rho) \\ 0 \end{bmatrix} \tag{59}$$

and

$$\hat{F}_a = \begin{bmatrix} 0 \\ A_f N_2 \end{bmatrix} = \begin{bmatrix} 0 \\ \hat{F}_2 \end{bmatrix} = F_a \tag{60}$$

Note that the system described in (56)-(60) above, is in the regular form similar to (10)-(12) in Section II.C. Therefore the observer design synthesis in Section II.D and II.E can also be used here.
A summary of the design method for sensor fault reconstruction is as follows:

1. Re-order the system such that the sensors prone to faults are in the lower half of the plant output vector as in (50).
2. Augment the system with the filtered version of the sensors prone to faults as in (53).
3. Replace the augmented plant outputs with the 'new' outputs, as (54).
4. Transform the augmented system using T_a defined in (55) so that in the new coordinates the output distribution matrix is as (56). (In actuator fault analysis the transformation matrix is T_o defined in Section II.C).
5. Transform the system using T_L as defined in (14).
6. Use the synthesis procedure in Section II.D and II.E to design the observer gains.
7. The gain in the original system is given by

$$G_l(\rho) = T_a^{-1} T_L^{-1} \tilde{G}_l(\rho), \; G_n = T_a^{-1} T_L^{-1} \tilde{G}_n \tag{61}$$

IV. Actuator fault reconstruction example

This section describes an application of the new theory described earlier. The LPV plant used in this section is obtained from[47] which was derived from software called FTLAB747, and represents the longitudinal axis motion of a large transport aircraft. The LPV plant was created using function substitution,[48] where the aerodynamic coefficients have been simplified by polynomial fitting from lookup tables obtained from NASA.[49,50] The aerodynamic coefficients are polynomial functions of velocity (V_{tas}) and angle of attack (α) for the range of [150, 250]m/s and [-2, 8]° respectively, at a fixed altitude of 7000m.[47] The LPV system states and inputs (for the LPV system given in[47]) are deviations from the trim values (i.e. $\bar{x} = x - x_{trim}$ and $\bar{u} = u - u_{trim}$). Further details of the LPV model description, trim values, validation, and a time response comparison (between the LPV and nonlinear models) can be found in.[47,48]

The states of the LPV plant in[47] are $[\bar{\alpha},\ \bar{q},\ \bar{V}_{tas},\ \bar{\theta},\ \bar{h}_e]^{\mathrm{T}}$ (which represent angle of attack, pitch rate, speed, pitch and altitude) and the inputs are $[\bar{\delta}_e,\ \bar{\delta}_s,\ \bar{T}_n]$ (which represent elevator, stabilizer and thrust). In this example, the outputs of the LPV plant are $[\bar{V}_{tas},\ \bar{\alpha},\ \bar{q}]^{\mathrm{T}}$. The LPV system given in[47] is obtained at trim values of

$$[\alpha_{trim},\ q_{trim},\ V_{tas_{trim}},\ \theta_{trim},\ h_{e_{trim}}] = [1.05^\circ,\ 0^\circ/s,\ 227.02m/s,\ 1.05^\circ,\ 7000m]$$

$$[\delta_{e_{trim}},\ \delta_{s_{trim}},\ T_{n_{trim}}] = [0.163^\circ,\ 0.590^\circ,\ 42291N]$$

For the observer design as proposed in this paper, the states have been reordered/transformed to regular form as in (12) and the state $\bar{h}_e$ has been removed. In regular form, the states become $[\bar{\theta},\ \bar{V}_{tas},\ \bar{\alpha},\ \bar{q}]^{\mathrm{T}}$ with inputs $[\bar{\delta}_e,\ \bar{\delta}_s,\ \bar{T}_n]$.

The LPV system matrices are given by

$$A(\rho) = A_0 + A_1\rho_1 + A_2\rho_2 + A_3\rho_3 + A_4\rho_4 + A_5\rho_5 + A_6\rho_6 + A_7\rho_7 \tag{62}$$

$$B(\rho) = B_0 + B_1\rho_1 + B_2\rho_2 + B_3\rho_3 + B_4\rho_4 + B_5\rho_5 + B_6\rho_6 + B_7\rho_7 \tag{63}$$

where

$$[\rho_1,\ \rho_2,\ \rho_3,\ \rho_4,\ \rho_5,\ \rho_6,\ \rho_7] := [\bar{\alpha},\ \bar{V}_{tas},\ \bar{V}_{tas}\bar{\alpha},\ \bar{V}_{tas}^2,\ \bar{V}_{tas}^2\bar{\alpha},\ \bar{V}_{tas}^3,\ \bar{V}_{tas}^4] \tag{64}$$

and $\bar{\alpha} = \alpha - \alpha_{trim}$, $\bar{V}_{tas} = V_{tas} - V_{tas_{trim}}$. Details of the matrices are given in the Appendix. In regular form, the LPV input distribution matrix is given by

$$B(\rho) = \begin{bmatrix} 0 & 0 & 0 \\ 0 & 0 & B_{23}(\rho) \\ B_{31}(\rho) & B_{32}(\rho) & B_{33}(\rho) \\ B_{41}(\rho) & B_{42}(\rho) & B_{43}(\rho) \end{bmatrix} \tag{65}$$

Here, it is assumed that the engine is fault free and the actuators to be monitored for faults comprise the elevator and stabilizer. Therefore the matrix $D(\rho)$ from (1) is given by

$$D(\rho) = \begin{bmatrix} 0 & 0 \\ 0 & 0 \\ B_{31}(\rho) & B_{32}(\rho) \\ B_{41}(\rho) & B_{42}(\rho) \end{bmatrix} \tag{66}$$

i.e. the first two columns of $B(\rho)$ in (65). The matrix $D(\rho)$ in (66) can be factorized as in (3) where

$$D(\rho) = \underbrace{\begin{bmatrix} 0 & 0 \\ 0 & 0 \\ 1 & 0 \\ 0 & 1 \end{bmatrix}}_{D} \underbrace{\begin{bmatrix} B_{31}(\rho) & B_{32}(\rho) \\ B_{41}(\rho) & B_{42}(\rho) \end{bmatrix}}_{E(\rho)} \tag{67}$$

IV.A. LPV Observer Design

The design of the observer gains are dependent on L_1 as shown in (47) and (14). In this example, L_1 is obtained using the MATLAB LMI multi-model state-feedback synthesis code 'msfsyn'[41] adapted to tackle an observer problem i.e. the dual of the standard control problem. (In fact, since $A_{11}(\rho)$ and $A_{211}(\rho)$ from (21) are scalar, the LMI code 'msfsyn'[41] can be used directly to obtain L_1.) Here, a simple pole placement design[41] has been selected to place the closed-loop poles inside the LMI region[41,45] in the complex plane to the left of the vertical line through -1. This yields $L_1 = 0.1533$. The range of V_{tas} and α is given by $[150,\ 250]$m/s and $[-2,\ 8]^\circ$ respectively.[47] As a result, T_L from (14) is given by

$$T_L = \begin{bmatrix} 1 & 0.1533 & 0 & 0 \\ 0 & 1 & 0 & 0 \\ 0 & 0 & 1 & 0 \\ 0 & 0 & 0 & 1 \end{bmatrix}$$

where for this example $T = I_3$. The stable design matrix $\tilde{A}^s_{22}$ has been chosen as $\tilde{A}^s_{22} = diag([-2,\ -3,\ -4])$ and therefore P_o from (25) is

$$P_o = \begin{bmatrix} 0.2500 & 0 & 0 \\ 0 & 0.1667 & 0 \\ 0 & 0 & 0.1250 \end{bmatrix}$$

Based on T_L above, the fixed gain G_n in (47) is given by

$$G_n = \begin{bmatrix} -0.1533 & 0 & 0 \\ 1 & 0 & 0 \\ 0 & 1 & 0 \\ 0 & 0 & 1 \end{bmatrix}$$

For simulation, the gain $G_l(\rho)$ in (23) has been split into varying and fixed components

$$G_l(\rho) = T_L^{-1}T_o^{-1}\tilde{G}_l(\rho) = T_L^{-1}T_o^{-1}\left(\begin{bmatrix} \tilde{A}_{12}(\rho) \\ \tilde{A}_{22}(\rho) \end{bmatrix} - \begin{bmatrix} 0 \\ \tilde{A}^s_{22} \end{bmatrix} \right) = G_{la}(\rho) - G_{lb}$$

where

$$G_{lb} = \begin{bmatrix} 0.3066 & 0 & 0 \\ -2 & 0 & 0 \\ 0 & -3 & 0 \\ 0 & 0 & -4 \end{bmatrix}$$

while

$$G_{la}(\rho) = G_{la_0} + G_{la_1}\rho_1 + G_{la_2}\rho_2 + G_{la_3}\rho_3 + G_{la_4}\rho_4 + G_{la_5}\rho_5 + G_{la_6}\rho_6 + G_{la_7}\rho_7$$

See the Appendix for details about the individual gains.

The 'equivalent output injection' signal[33] $\nu_{eq}(t)$ can be approximated to any degree of accuracy by replacing (25) with

$$\nu_{eq}(t) = -\mathcal{K}(t, y, u, \rho)\|\tilde{D}_2\|\frac{P_o e_y}{\|P_o e_y\| + \delta} \tag{68}$$

The variable δ is a small scalar which is used to smooth the sign function and provide extra degrees of freedom in terms of the tradeoff between robustness and chattering.[24] Here, δ has been chosen as 0.001 and the modulation gain $\mathcal{K}(t, y, u, \rho)$ was chosen as -10.

IV.B. Actuator Faults Reconstruction Results

IV.B.1. Simulations using LPV model

A closed-loop controller has been used to provide a simulation in which altitude is maintained (the LPV model assumes a fixed altitude) and a good response to a change in speed is obtained. The controller is based on the reconfigurable LPV control design[20] for the longitudinal axis, which is the baseline controller given in the FTLAB747-V6.1/6.5 software and is described in detail in.[20] The controlled outputs are flight path angle (γ) and speed. The controller uses the elevators and thrust for flight manoeuvres, while the stabilizer is used to trim the aircraft.[20] The controller was designed to deal with elevator faults (and failures). (Note that although it was shown in[20] that an elevator failure was considered – and uses the stabilizer as redundancy – this is not implemented in the FTLAB747-V6.1/6.5 software and therefore is not considered in the example in this paper).

The faults in this paper are simulated as additive perturbations occurring in the actuator inputs, and unknown to the observer. The additive fault is considered to simplify the analysis of the fault reconstruction performance. Such an approach is also considered in[15] for example.

Figure 1 shows the simulation of the LPV plant with a stabilizer fault. Figure 1(c) shows the actual faults added to the stabilizer. Figure 1(b) shows the deflections of the stabilizer with the added fault, together with the elevator deflections counteracting the effect of the faulty stabilizer to maintain the desired flight path angle γ and speed V_{tas} tracking. The tracking performance is shown in Figure 1(a). Figure 1(c) shows a good reconstruction of the fault while maintaining the sliding motion (e_y close to zero).

Figure 2 shows the simulation of the LPV plant with an elevator fault. Figure 2(a) shows no degradation in the tracking performance. Figure 2(b) shows that the controller manages to compensate for the fault in the actuators and thus the effect of the additive fault does not appear in the elevator deflection, while the stabilizer is in the trim position. Figure 2(c) shows a good reconstruction of the elevator faults, and that the sliding motion is maintained.

IV.B.2. Simulation using nonlinear model

The nonlinear simulations associated with the same scenario as in Section IV.B.1 were conducted using the FTLAB747-V6.1/6.5 software which runs under MATLAB and SIMULINK. This software represents a realistic 6-DOF model of a large civil transport aircraft with aerodynamic coefficients provided by NASA[49,50] and realistic actuator dynamics and limits. The overall model contains 77 states including the actuator and sensor dynamics. This software has been used by many researchers as a platform to test FDI and FTC schemes (see for example references[6,15,51–53]). The software has been developed and enhanced over the years by van der Linden,[54] Smaili[55] and Marcos & Balas.[42] Recently a version of this software has been used in the Group for aeronautical research and technology in Europe (GARTEUR) FM-AG16 as a benchmark model[43] to study modern fault tolerant control schemes (See for example references[56–60] for publications from this group).

Note that the LPV model used above was also derived from this software. The controller which was used in the LPV model test is also considered here to maintain altitude and to react to demand changes in speed. The nonlinear simulation is conducted with trim conditions of

$$[\alpha_{trim},\ q_{trim},\ V_{tas_{trim}},\ \theta_{trim},\ h_{e_{trim}}]^{\mathrm{T}} = [1.8^\circ,\ 0^\circ/s,\ 227.02m/s,\ 1.8^\circ,\ 7000m]$$

$$[\delta_{e_{trim}},\ \delta_{s_{trim}},\ T_{n_{trim}}] = [0.5895^\circ,\ 0.0591^\circ,\ 40863N]$$

Note that this is not exactly the same trim values used to obtain the LPV model in.[47] This is due to the fact that some of the trim configurations are not available in[47] (e.g. the initial mass and the x_{cg} location). The above trim was obtained with an initial mass of 300,000kg, $x_{cg} = 25\%mac$ and 1.085° pilot column deflection.

Figure 3 shows the simulation results from using the nonlinear plant with elevator faults, with the same LPV observer as in the previous subsection. As in the LPV tests, the faults are simulated as additive perturbations at the actuator level and are unknown to the observer. Figure 3(a) shows the demanded change in speed and the speed tracking performance. There is a zero demand on γ (to maintain altitude around 7000m). Figure 3(a) shows good tracking performance even in the presence of the elevator fault. Figure 3(b) shows that the controller has managed to compensate for the additive fault which does not

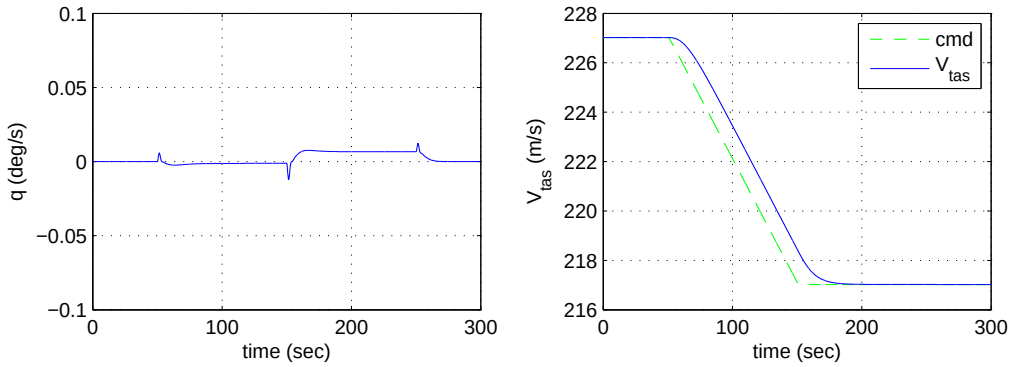

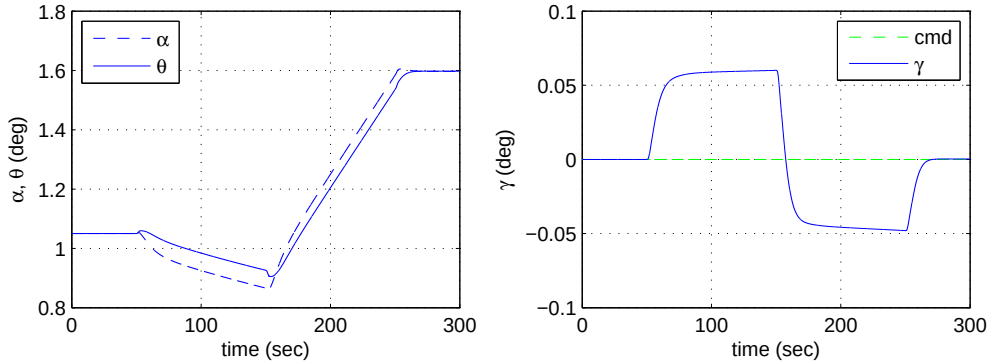

(a) states

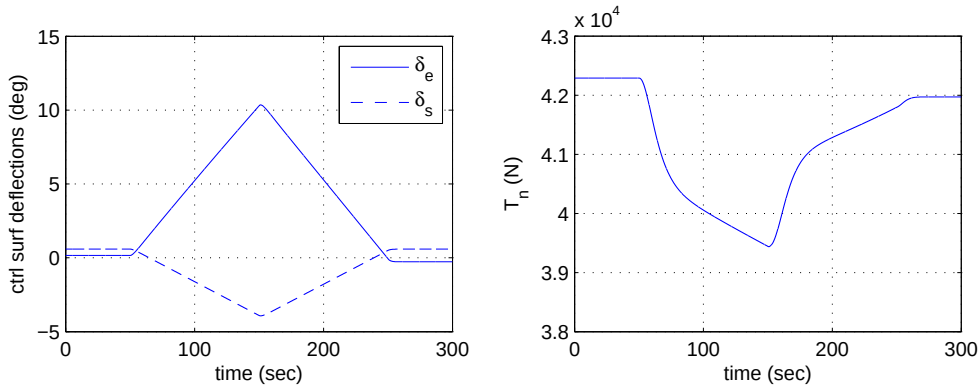

(b) control surface deflections

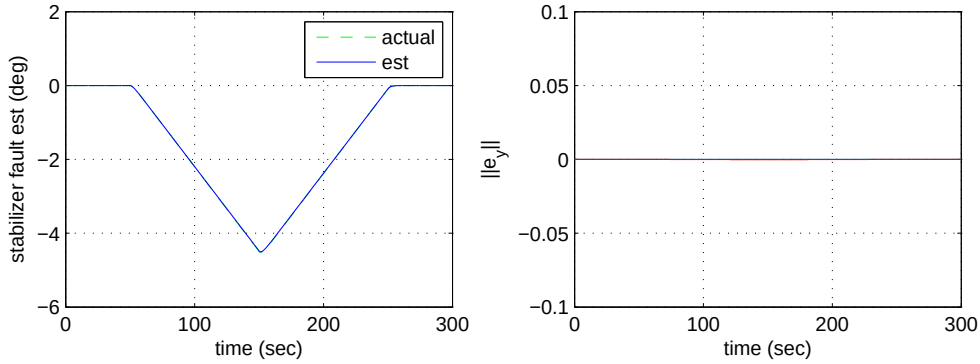

(c) fault reconstructions & observer errors

Figure 1. LPV model simulation: stabilizer fault

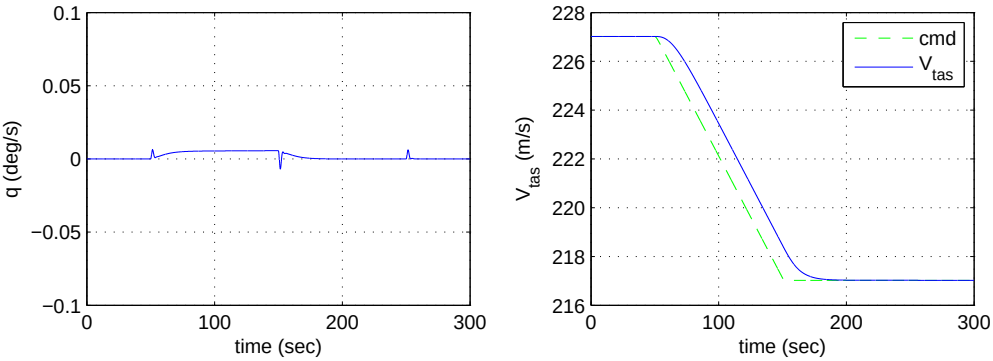

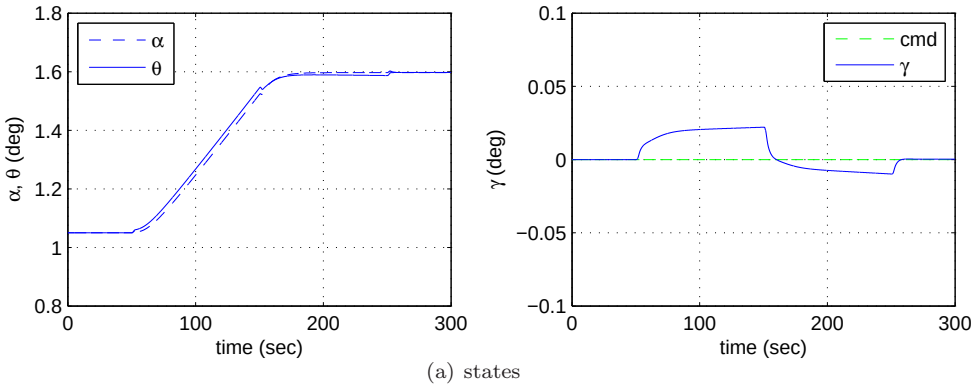

(a) states

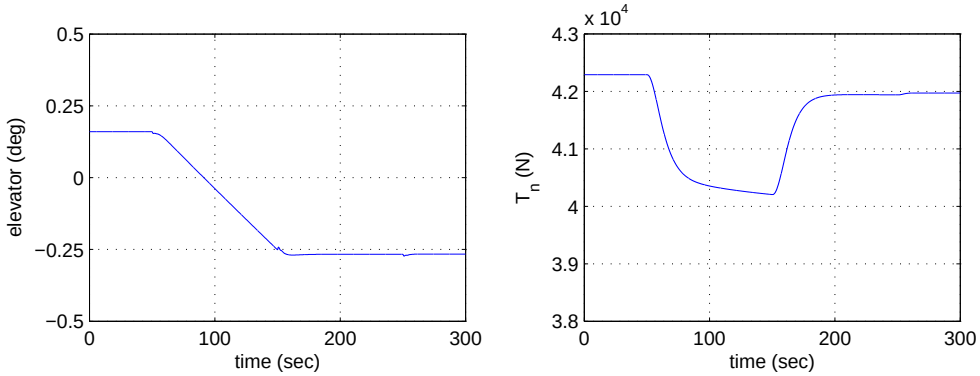

(b) control surface deflections

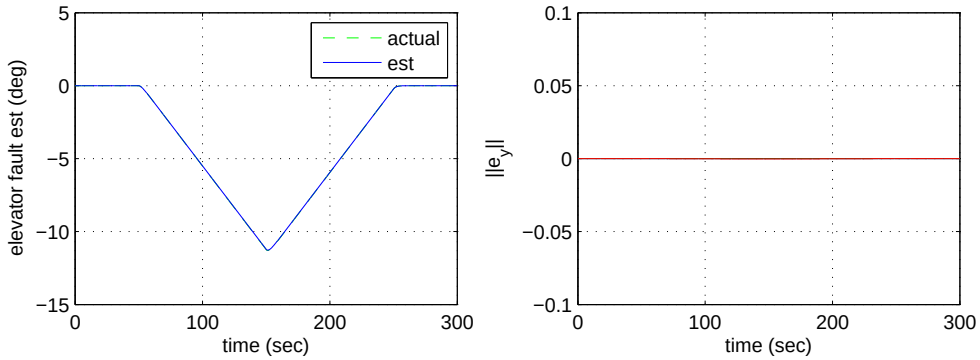

(c) fault reconstructions & observer errors

Figure 2. LPV model simulation: elevator fault

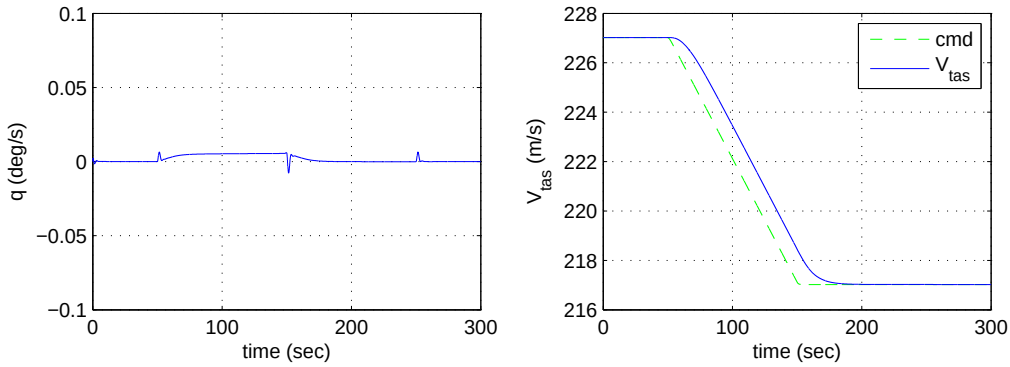

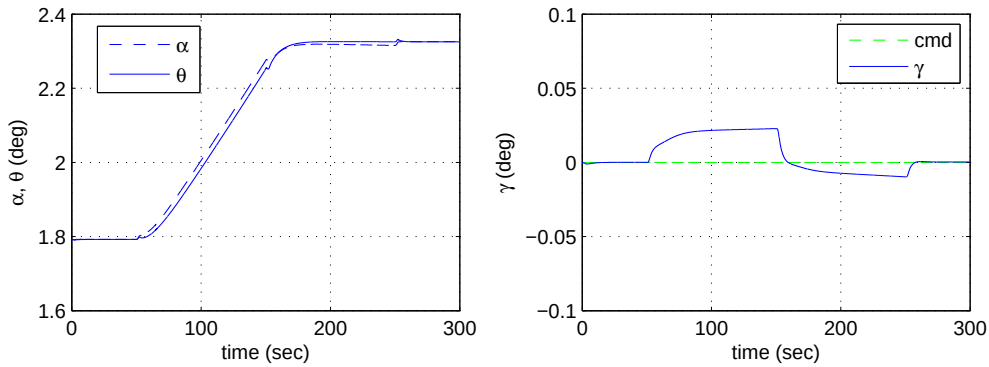

(a) states

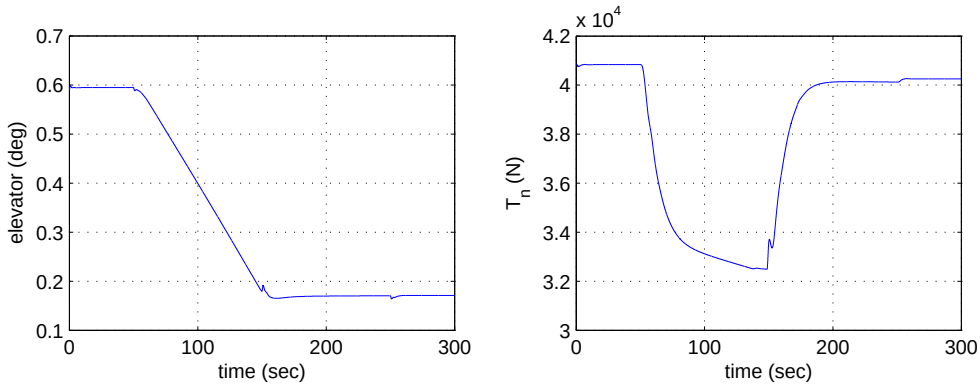

(b) control surface deflections

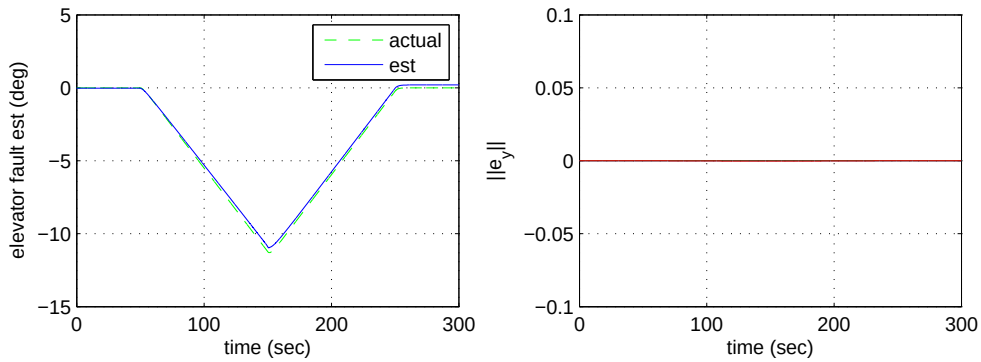

(c) fault reconstructions & observer errors

Figure 3. Nonlinear model simulation: elevator fault

appear in the elevator deflection. Figure 3(c) shows the sliding motion. This figure also shows a good reconstruction of the fault by the proposed observer scheme.

Note that the fault reconstruction is good but not perfect. One contributing factor to the mismatch relates to the quality of the LPV model used to represent the actual nonlinear model. Longitudinal excitation (using the elevator) of the open loop LPV and the nonlinear plant in,[47] shows some difference in the dynamical behaviour. This is due to the approximations used to obtain the LPV model (e.g. the approximations from the polynomial fit of the aerodynamic coefficients, $1/V_{tas}$ which is approximated by a Taylor series, and the approximations $(sin(\alpha) \approx \alpha, sin(\theta) \approx \theta, cos(\alpha) \approx 1, cos(\theta) \approx 1))$ which are used to obtained the LPV model. A much better LPV model for FDI is given in,[15] however this model is not available in the open literature. Another contributing factor is the non-matching trim conditions used for the simulation, and the ones used to obtain the LPV model.

Future work involves the design of a robust LPV observer to improve the fault reconstructions, which mitigates the LPV model nonlinear plant mismatch.

V. Sensor faults reconstruction example

As in Section IV.B, the simulations associated with the sensor fault reconstruction is first tested on the LPV model,[47] and then tested on the full high-fidelity nonlinear model using FTLAB747.[42]

V.A. LPV Observer Design

In this example, it will be assumed that the θ measurement is prone to faults. The system states have been reordered to $x(t) = [\alpha,\ q,\ V_{tas},\ \theta]$, so that θ appears at the bottom of the output vector: specifically

$$y(t) = \left[\begin{array}{c} \alpha(t) \\ q(t) \\ \hline V_{tas}(t) \\ \hline \theta(t) \end{array}\right] \begin{array}{l} \Big\} \text{fault free} \\ \\ \} \text{prone to fault} \end{array} = \begin{array}{l} C_1 \Big\{ \\ \\ C_2 \{ \end{array} \underbrace{\left[\begin{array}{cccc} 1 & 0 & 0 & 0 \\ 0 & 1 & 0 & 0 \\ \hline 0 & 0 & 1 & 0 \\ \hline 0 & 0 & 0 & 1 \end{array}\right]}_{C} x(t) + \begin{array}{l} \\ \\ N_2 \{ \end{array} \underbrace{\left[\begin{array}{c} 0 \\ 0 \\ \hline 0 \\ \hline 1 \end{array}\right]}_{N} F_o(t)$$

where $N_2 = 1$. The scalar variable A_f (in this case) which defines the filter in (51) has been chosen as $A_f = 1$. The fixed components of the augmented system in (53) are

$$A_f C_2 = \left[\begin{array}{cccc} 0 & 0 & 0 & 1 \end{array}\right],\ -A_f = -1,\ A_f N = -1$$

The new augmented system output in (54) is

$$\underbrace{\left[\begin{array}{c} y_1(t) \\ \hline z_f(t) \end{array}\right]}_{y_a} = \underbrace{\left[\begin{array}{ccccc} 1 & 0 & 0 & 0 & 0 \\ 0 & 1 & 0 & 0 & 0 \\ 0 & 0 & 1 & 0 & 0 \\ \hline 0 & 0 & 0 & 0 & 1 \end{array}\right]}_{C_a} \underbrace{\left[\begin{array}{c} x(t) \\ \hline z_f(t) \end{array}\right]}_{x_a} \tag{69}$$

The transformation matrix T_a from (55) is

$$T_a = \left[\begin{array}{cccc|c} 0 & 0 & 0 & 1 & 0 \\ 1 & 0 & 0 & 0 & 0 \\ 0 & 1 & 0 & 0 & 0 \\ 0 & 0 & 1 & 0 & 0 \\ \hline 0 & 0 & 0 & 0 & 1 \end{array}\right] \tag{70}$$

This brings about the canonical form in (56)-(60).

As in Section IV.A, $L_{1_{aug}}$ is obtained using the code 'msfsyn' adapted to tackle an observer problem (Here $A_{11}(\rho)$ from (21) is a scalar and $A_{211}(\rho)$ is a 3×1 matrix, whose transpose is used in the code 'msfsyn'[41] as

the input distribution matrix). A simple pole placement design[41] has been selected to place the closed-loop poles inside the LMI region[41,45] to the left of a vertical line through -1. This yields $L_{1_{aug}} = [0\ 0\ 0.1533]$. The range of $\bar{V}_{tas}$ and $\bar{\alpha}$ is given in Section IV.A. The transformation matrix T_L from (14) is given by

$$T_{L_{aug}} = \begin{bmatrix} 1 & 0 & 0 & 0.1533 & 0 \\ 0 & 1 & 0 & 0 & 0 \\ 0 & 0 & 1 & 0 & 0 \\ 0 & 0 & 0 & 1 & 0 \\ 0 & 0 & 0 & 0 & 1 \end{bmatrix}$$

The stable design matrix $\tilde{A}^s_{22}$ has been chosen as $\tilde{A}^s_{22} = diag([-2,\ -3,\ -4,\ -5])$ and $P_{o_{aug}}$ from (25) is

$$P_{o_{aug}} = \begin{bmatrix} 0.2500 & 0 & 0 & 0 \\ 0 & 0.1667 & 0 & 0 \\ 0 & 0 & 0.1250 & 0 \\ 0 & 0 & 0 & 0.1000 \end{bmatrix}$$

The fixed gain $G_{n_{aug}}$ in (47) is given by

$$G_{n_{aug}} = \begin{bmatrix} 1.0000 & 0 & 0 & 0 \\ 0 & 1.0000 & 0 & 0 \\ 0 & 0 & 1.0000 & 0 \\ 0 & 0 & -0.1533 & 0 \\ 0 & 0 & 0 & 1.0000 \end{bmatrix}$$

As in Section IV.A, the gain $G_{l_{aug}}(\rho)$ in (23) has been split into varying and fixed components

$$G_{l_{aug}}(\rho) = T_L^{-1}T_a^{-1}\tilde{G}_l(\rho) = T_L^{-1}T_a^{-1}\left(\begin{bmatrix} \tilde{A}_{12}(\rho) \\ \tilde{A}_{22}(\rho) \end{bmatrix} - \begin{bmatrix} 0 \\ \tilde{A}^s_{22} \end{bmatrix} \right) = G_{la_{aug}}(\rho) - G_{lb_{aug}}$$

where

$$G_{lb_{aug}} = \begin{bmatrix} -2.0000 & 0 & 0 & 0 \\ 0 & -3.0000 & 0 & 0 \\ 0 & 0 & -4.0000 & 0 \\ 0 & 0 & 0.6132 & 0 \\ 0 & 0 & 0 & -5.0000 \end{bmatrix}$$

and

$$G_{la_{aug}}(\rho) = G_{la_{aug0}} + G_{la_{aug1}}\rho_1 + G_{la_{aug2}}\rho_2 + G_{la_{aug3}}\rho_3 + G_{la_{aug4}}\rho_4 + G_{la_{aug5}}\rho_5 + G_{la_{aug6}}\rho_6 + G_{la_{aug7}}\rho_7$$

See the Appendix for details of the individual gains.

The 'output injection signal' (25) has been approximated as in (68). The gain $\mathcal{K}_{aug}(t, y, u, \rho)$ was chosen as -10 and δ_{aug} was chosen as 0.001.

V.B. Sensor Faults Reconstruction Results

V.B.1. Simulations using LPV model

The controller used in Section IV.B.1, was used here to maintain altitude ($\gamma_{cmd} = 0$) and effect a demand change in speed ($V_{tas} \neq 0$). Again the trim values are not considered in the plots.

It is assumed that the sensor fault only affects the fault monitoring unit (i.e. the faulty measurement only appears before the FDI observer) and the faulty sensor (in this case θ) measurement is not used by the controller for feedback control. Here, the sensor fault is simulated as an additive fault.

Figure 4 shows the results on the LPV plant. Figure 4(a) shows the observer states (the actual measurements from the plant are not shown). Figure 4(c) shows the errors between the actual measurements

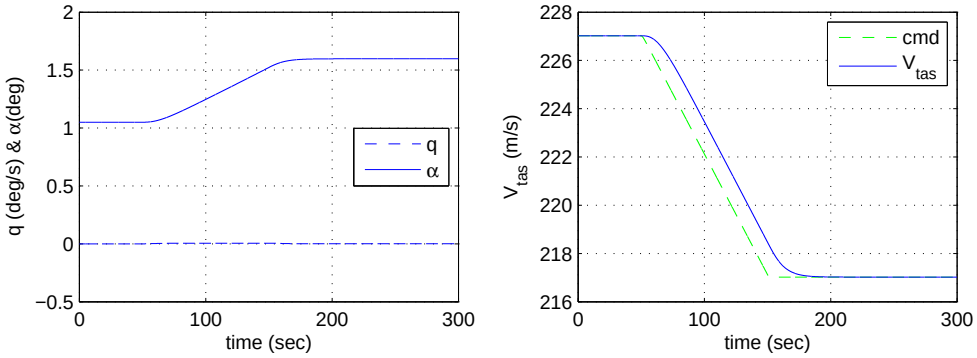

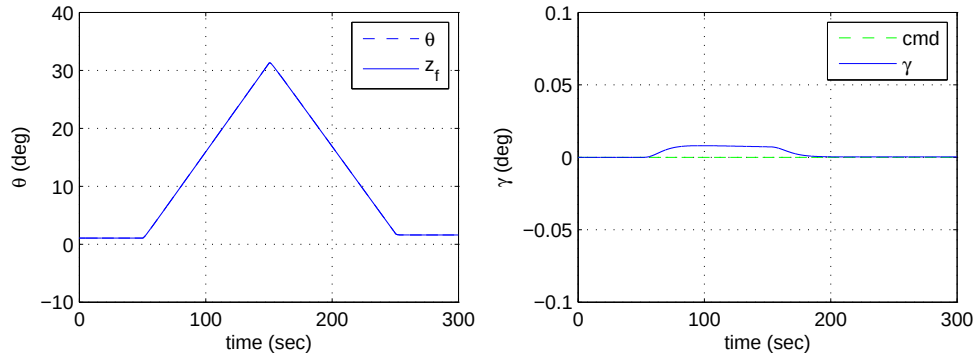

(a) observer states

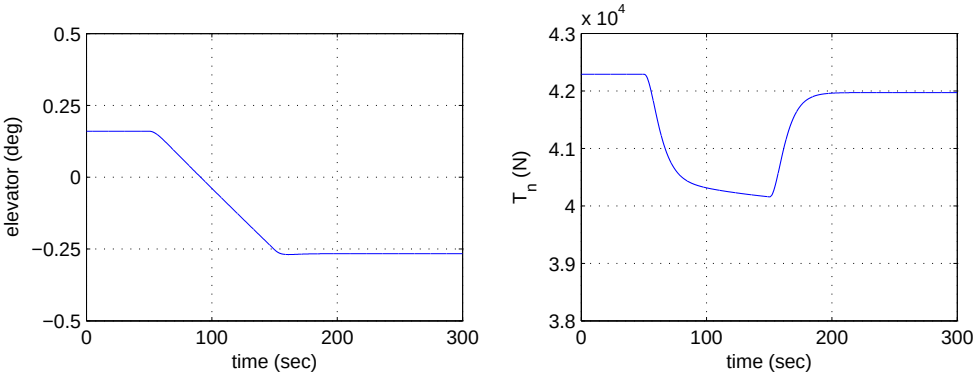

(b) control surface deflections

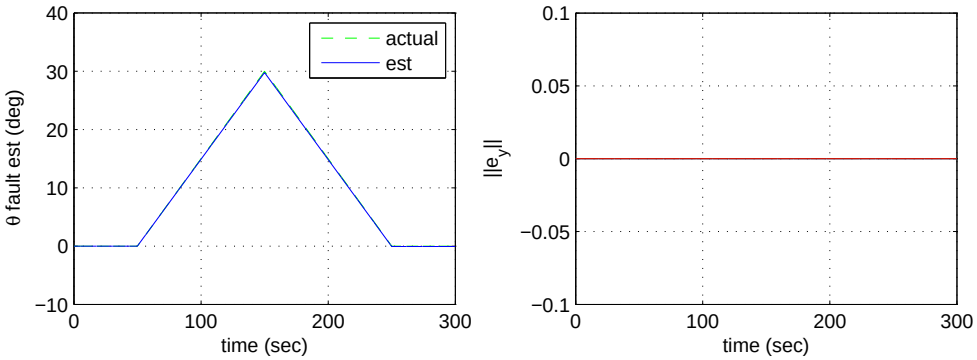

(c) fault reconstructions & observer errors

Figure 4. LPV model simulation: θ fault

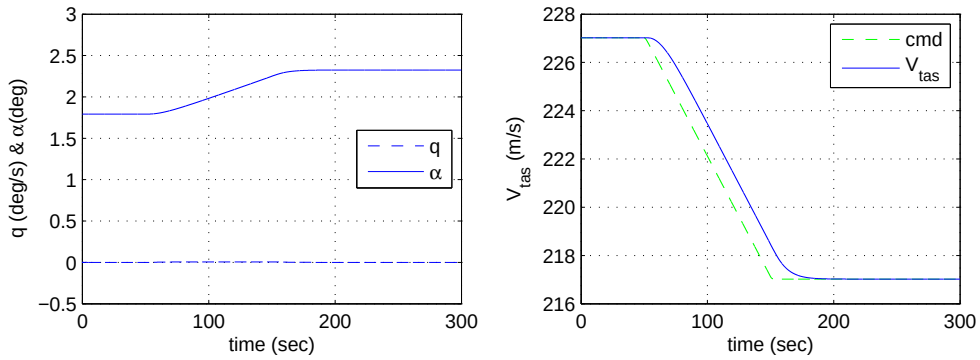

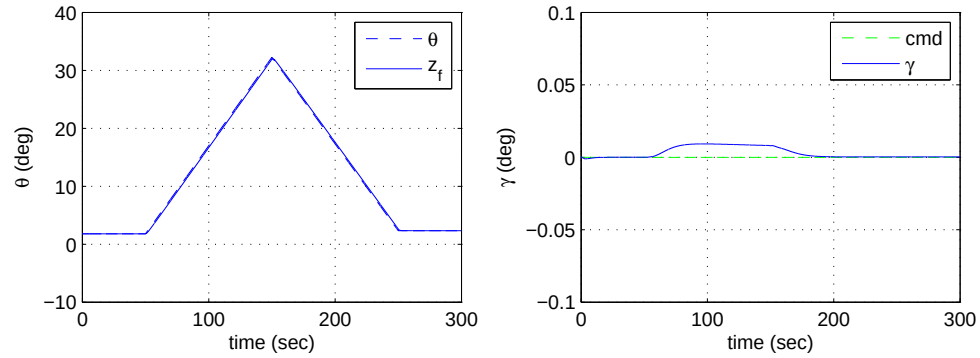

(a) observer states

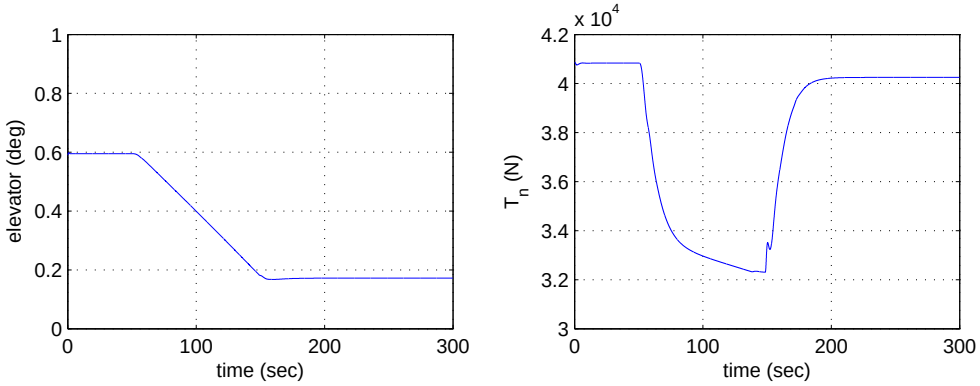

(b) control surface deflections

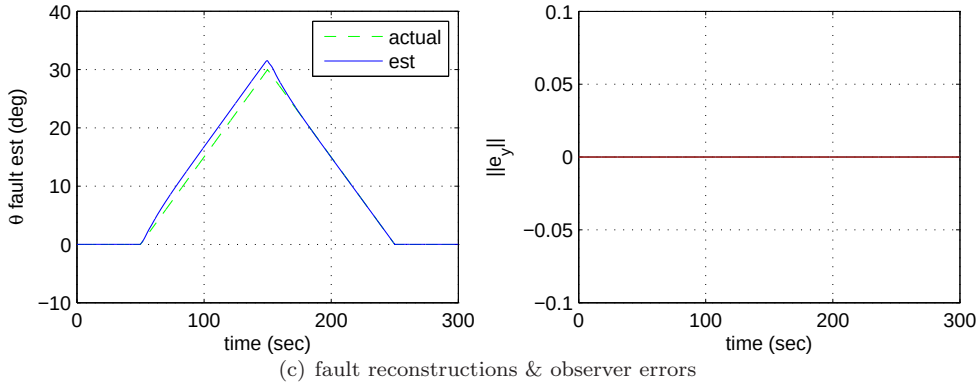

(c) fault reconstructions & observer errors

Figure 5. Nonlinear model simulation: θ fault

and the observer states are very small, indicating good estimates of the states and the existence of a sliding motion. Figure 4(a) shows the demand change in V_{tas} and no change in γ. Figure 4(a) shows the corrupted measurement of θ and its filtered version z_f. Note that the effect of the filter is not visible (both θ and z_f overlap). Finally Figure 4(c) shows a good reconstruction of fault.

V.B.2. Simulation using nonlinear model

The same controller as used in the previous simulation tests has been used here. As in Section V.B.1, the sensor fault only affects the fault monitoring unit. The simulation test for the LPV plant, as in Section V.B.1, is repeated here for the nonlinear test using the FTLAB747-V6.1/6.5 software.

Figure 5 shows the results of repeating the same tests and manoeuvres on the nonlinear model. Figure 5(a) shows the observer states. Figure 5(c) shows only very small errors between the actual measurements and the observer states. This shows good state estimation and the existence of a sliding motion – thus indicating good performance of the observer when simulated on the nonlinear plant. Figure 5(c) also shows good reconstruction of the faults. A small degradation in the fault estimate can be seen during the decrease in speed between 50-150sec. As the speed settles at -20m/s slower than the trim, there is no degradation in the fault reconstruction.

VI. Conclusions

This paper has proposed a new LPV based sliding mode observer for reconstruction of both actuator and sensor faults. For actuator faults, the design involves factorizing the varying input distribution matrix into a fixed and varying part, and designing gains for the 'virtual' system. The fixed nonlinear and varying linear observer gains, are dependant on a coordinate transformation which ensures a stable reduced order sliding motion in the state estimation error space using LMI methods. The virtual actuator fault reconstructions are based on the 'equivalent output error injection signals' of the observer system, and are mapped into the actual faults by considering the factorization of the input distribution matrix. For sensor faults, the observer design involves re-formulating the sensor fault reconstruction problem into an actuator fault reconstruction problem. This allows the observer design synthesis approach for the actuator faults to be applied directly for designing the sensor fault scheme. The simulation results for both actuator and sensor faults on the LPV and the high fidelity nonlinear plant representing a large transport aircraft show good reconstructions of the faults, demonstrating the capability of the proposed schemes.

References

[1]Patton, R., "Robustness in model-based fault diagnosis: the 1997 situation," *IFAC Annual Reviews*, Vol. 21, 1997, pp. 101–121.

[2]Zhang, Y. and Jiang, J., "Bibliographical review on reconfigurable fault tolerant control systems," *Proceedings of the IFAC Symposium SAFEPROCESS '03, Washington*, 2003, pp. 265–276.

[3]Alcorta-Garcia, E., Zolghadri, A., and Goupil, P., "A Novel Non-Linear Observer-Based Approach To Osilatory Failure Detection," *European Control Conference*, 2009, pp. 1901–1906.

[4]Amato, F., Mattei, M., Iervolino, R., and Paviglianiti, G., "A Nonlinear UIO Scheme For The FDI On A Small Commercial Aircraft," *IEEE International Conference on Control Applications*, 2002, pp. 235–240.

[5]Castaldi, P., Geri, W., Bonfé, M., Simani, S., and Benini, M., "Design of residual generators and adaptive filters for the FDI of aircraft model sensors," *Control Engineering Practice*, , No. doi:10.1016/j.conengprac.2008.11.006, 2009.

[6]Marcos, A., Ganguli, S., and Balas, G. J., "An application of H_∞ fault detection and isolation to a transport aircraft," *Control Engineering Practice*, Vol. 13, No. 1, 2005, pp. 105–119.

[7]Chen, J. and Patton, R. J., *Robust Model-Based Fault Diagnosis for Dynamic Systems*, Kluwer Academic Publishers, 1999.

[8]Wu, N. E., Zhang, Y., and Zhou, K., "Control effectiveness estimation using an adaptive Kalman estimator," *Proceedings of the 1998 IEEE International Symposium on Intelligent Control (ISIC) held jointly with IEEE International Symposium on Computational Intelligence in Robotics and Automation (CIRA) Intelligent Systems and Semiotics (ISAS)*, 1998, pp. 181–6.

[9]Balas, G. J., "Linear, parameter–varying control and its application to a turbofan engine," *International Journal of Robust and Nonlinear Control*, Vol. 12, 2002, pp. 763–796.

[10]Bokor, J. and Balas, G., "Detection filter design for LPV systems - A geometric approach," *Automatica*, Vol. 40, 2004, pp. 511–518.

[11]Hallouzi, R., Verdult, V., Babuska, R., and Verhaegen, M., "Fault Detection and Identification of Actuator Faults Using Linear Parameter Varying Models," *Preprints of the IFAC World Congress*, 2005.

[12]Bokor, J., Szabo, Z., and Stikkel, G., "Failure Detection For Quasi LPV Systems," *IEEE Conference on Decision and Control*, 2002.

[13]Grenaille, S., Henry, D., and Zolghadri, A., "A Method for Designing Fault Diagnosis Filters for LPV Polytopic Systems," *Journal of Control Science and Engineering*, , No. doi:10.1155/2008/231697, 2008.

[14]Armeni, S., Casavola, A., and Mosca, E., "Robust fault detection and isolation for LPV systems under a sensitivity constraint," *International Journal Of Adaptive Control And Signal Processing*, Vol. 23, 2009, pp. 55–72.

[15]Szaszi, I., Marcos, A., Balas, G. J., and Bokor, J., "Linear parameter-varying detection filter design for a Boeing 747-100/200 aircraft," *Journal of Guidance, Control, and Dynamics*, Vol. 28, No. 3, 2005, pp. 461–470.

[16]Becker, G., Packard, A., Philbrick, D., and Balas, G., "Control of Parametrically-Dependent Linear Systems A Single Quadratic lyapunov approach," *American Control Conference*, 1993, pp. 2795–99.

[17]Apkarian, P., Gahinets, P., and Becker, G., "Self-scheduled $\mathcal{H}_\infty$ Control of Linear Parameter-varying Systems: a Design Example," *Automatica*, Vol. 31, No. 9, 1995, pp. 1251–1261.

[18]Wu, F., *Control of Linear Parameter Varying systems*, Ph.D. thesis, University of California at Berkeley, 1995.

[19]Papageorgiou, G., *Robust Control Systems Design H-Infinity Loop Shaping And Aerospace Applications*, Ph.D. thesis, University of Cambridge, 1998.

[20]Ganguli, S., Marcos, A., and Balas, G. J., "Reconfigurable LPV control design for Boeing 747-100/200 longitudinal axis," *American Control Conference*, 2002, pp. 3612–3617.

[21]Casavola, A., Famularo, D., Franz, G., and Sorbara, M., "A fault-detection, filter-design method for linear parameter-varying systems," *Proceedings of the Institution of Mechanical Engineers, Part I: Journal of Systems and Control Engineering*, Vol. 221, No. 6, 2007, pp. 865–874.

[22]Sato, M., "Filter design for LPV systems using quadratically parameter-dependent Lyapunov functions," *Automatica*, Vol. 42, No. 11, 2006, pp. 2017–2023.

[23]Henry, D., Falcoz, A., and Zolghadri, A., "Structured H_∞/H_- LPV filters for fault diagnosis: Some new results," *Proceedings of the IFAC Symposium SAFEPROCESS '09, Barcelona*, 2009, pp. 420–425.

[24]Edwards, C. and Spurgeon, S. K., *Sliding Mode Control: Theory and Applications*, Taylor & Francis, 1998.

[25]Hermans, F. and Zarrop, M., "Sliding mode observers for robust sensor monitoring," *Proceedings of the 13th IFAC World Congress*, 1996, pp. 211–216.

[26]Yang, H. and Saif, M., "Fault detection in a class of nonlinear systems via adaptive sliding observer," *Proceedings of the IEEE International Conference on Systems, Man and Cybernetics*, 1995, pp. 2199–2204.

[27]Zhang, Y. M. and Jiang, J., "Active fault-tolerant control system against partial actuator failures," *IEE Proceedings: Control Theory & Applications*, Vol. 149, 2002, pp. 95–104.

[28]Kim, Y. W., Rizzoni, G., and Utkin, V., "Developing a fault tolerant power train system by integrating the design of control and diagnostics," *International Journal of Robust and Nonlinear Control*, Vol. 11, 2001, pp. 1095–1114.

[29]Edwards, C. and Tan, C. P., "Sensor fault tolerant control using sliding mode observers," *Control Engineering Practice*, Vol. 16, 2006, pp. 897–908.

[30]Alwi, H. and Edwards, C., "Fault Detection and Fault-Tolerant Control of a Civil Aircraft Using a Sliding-Mode-Based Scheme," *IEEE Transactions on Control Systems Technology*, Vol. 16, No. 3, 2008, pp. 499–510.

[31]Wu, N. E., Zhang, Y., and Zhou, K., "Detection, estimation, and accommodation of loss of control effectiveness," *International Journal of Adaptive Control and Signal Processing*, Vol. 14, 2000, pp. 775–95.

[32]Zhang, Y. and Jiang, J., "Design of integrated fault detection, diagnosis and reconfigurable control systems," *Proceedings of the IEEE Conference on Decision and Control*, 1999, pp. 3587–3592.

[33]Edwards, C., Spurgeon, S., and Patton, R., "Sliding Mode Observers for Fault Detection," *Automatica*, Vol. 36, 2000, pp. 541–553.

[34]Tan, C. P. and Edwards, C., "An LMI approach for designing sliding mode observers," Department of Engineering Report 00–1, Leicester University, 2000.

[35]Tan, C. P. and Edwards, C., "Sliding Mode Observers for Robust Detection and Reconstruction of Actuator and Sensor Faults," *International Journal of Robust and Nonlinear Control*, Vol. 13, 2003, pp. 443–463.

[36]Yan, X. G. and Edwards, C., "Nonlinear robust fault reconstruction and estimation using a sliding mode observer," *Automatica*, Vol. 43, No. 9, 2007, pp. 1605–1614.

[37]Sivrioglu, S. and Nonami, K., "Sliding Mode Control With Time-Varying Hyperplane for AMB Systems," *IEEE/ASME Transactions On Mechatronics*, Vol. 3, No. 1, 1998, pp. 51–59.

[38]Nonami, K. and Sivrioglu, S., *Variable structure systems, sliding mode and nonlinear control*, Vol. 247, chap. Sliding mode control with gain scheduled hyperplane for LPV plant, Springer-Verlag, 1999, pp. 263–279.

[39]Xie, W. and Eisaka, T., "Design of LPV control systems based on Youla parameterisation," *IEE Proc., Control Theory Applications*, Vol. 151, No. 4, 2004, pp. 465472.

[40]de Oca, S. M., Puig, V., Theilliol, D., and Tornil-Sin, S., "Fault-Tolerant Control Design using LPV Admissible Model Matching: Application to a Two-degree of Freedom Helicopter," *17th Mediterranean Conference on Control & Automation*, 2009, pp. 522–527.

[41]Gahinet, P., Nemirovski, A., Laub, A., and Chilali, M., *LMI Control Toolbox, User Guide*, MathWorks, Inc., 1995.

[42]Marcos, A. and Balas, G. J., "A Boeing 747–100/200 Aircraft Fault Tolerant and Diagnostic Benchmark," Tech. Rep. AEM–UoM–2003–1, Department of Aerospace and Engineering Mechanics, University of Minnesota, 2003.

[43]Smaili, M. H., Breeman, J., Lombaerts, T. J. J., and Joosten, D. A., "A simulation benchmark for integrated fault tolerant flight control evaluation," *AIAA Modeling and Simulation Technologies Conference and Exhibit*, 2006.

[44]Tan, C. P. and Edwards, C., "An LMI Approach for Designing Sliding Mode Observers," *International Journal of Control*, Vol. 74, 2001, pp. 1559–1568.

[45]Chilali, M. and Gahinet, P., "$\mathcal{H}_\infty$ design with pole placement constraints: an LMI approach," *IEEE Transactions on Automatic Control*, Vol. AC-41, 1996, pp. 358–367.

[46]Tan, C. and Edwards, C., "Sliding Mode Observers for Reconstruction of Simultaneous Actuator and Sensor Faults," *Proceedings of the Conference on Decision and Control, CDC '03, Hawaii*, 2003, pp. 1455–1460.

[47]Khong, T. H. and Shin, J., "Robustness Analysis of Integrated LPV-FDI Filters and LTI-FTC System for a Transport Aircraft," *AIAA Guidance, Navigation and Control Conference and Exhibit*, No. AIAA 2007-6771, 2007.

[48]Marcos, A. and Balas, G. J., "Development of Linear-Parameter-Varying Models for Aircraft," *AIAA Journal of Guidance, Control and Dynamics*, Vol. 27, No. 2, 2004, pp. 218–228.

[49]Hanke, C. and Nordwall, D., "The simulation of a Jumbo Jet Transport Aircraft. Volume II: Modelling Data," Tech. Rep. CR-114494/D6-30643-VOL2, NASA and The Boeing Company, 1970.

[50]Hanke, C., "The simulation of a Large Jet Transport Aircraft. Volume I: Mathematical Model," Tech. Rep. CR-1756, NASA and the Boeing company, 1971.

[51]Hennig, A. and Balas, G. J., "MPC Supervisory Flight Controller: A Case Study to Flight EL AL 1862," *AIAA Guidance, Navigation and Control Conference and Exhibit*, 2008.

[52]Marcos, A. and Balas, G. J., "A robust integrated controller/diagnosis aircraft application," *International Journal of Robust and Nonlinear Control*, Vol. 15, No. 12, 2005, pp. 531–551.

[53]Zhou, K., Rachinayani, P. K., Liu, N., Ren, Z., and Aravna, J., "Fault Diagnosis and Reconfigurable Control for Flight Control Systems with Actuator Failures," *43rd IEEE Conference on Decision and Control, Bahamas*, 2004.

[54]van der Linden, C. A. A. M., "DASMAT: Delft University aircraft simulation model and analysis tool," Tech. Rep. LR–781, Technical University of Delft, the Netherlands, 1996.

[55]Smaili, M. H., "FLIGHTLAB 747: Benchmark for Advance Flight Control Engineering," Tech. rep., Technical University Delft, the Netherlands, 1999.

[56]Stroosma, O., Smaili, H., Lombaerts, T., and Mulder, J. A., "Piloted Simulator Evaluation of New Fault-Tolerant Flight Control Algorithms for Reconstructed Accident Scenarios," *AIAA Modeling and Simulation Technologies Conference and Exhibit*, 2008.

[57]Lombaerts, T. J. J., Huisman, H. O., Chu, Q. P., Mulder, J. A., and Joosten, D. A., "Flight Control Reconfiguration based on Online Physical Model Identification and Nonlinear Dynamic Inversion," *AIAA Guidance, Navigation and Control Conference and Exhibit*, No. AIAA 2008-7435, 2008.

[58]Cieslak, J., Henry, D., Zolghadri, A., and Goupil, P., "Development of an Active Fault-Tolerant Flight Control Strategy," *AIAA Journal of Guidance, Control and Dynamics*, Vol. 31, No. 1, 2008, pp. 135–147.

[59]Hallouzi, R. and Verhaegen, M., "Fault-Tolerant Subspace Predictive Control Applied to a Boeing 747 Model," *AIAA Journal of Guidance, Control and Dynamics*, Vol. 31, No. 4, 2008, pp. 873–883.

[60]Alwi, H., Edwards, C., Stroosma, O., and Mulder, J. A., "Fault Tolerant Sliding Mode Control Design with Piloted Simulator Evaluation," *AIAA Journal of Guidance, Control and Dynamics*, Vol. 31, No. 5, 2008, pp. 1186–1201.

VII. Appendix

VII.A. The LPV matrices $A(\rho), B(\rho)$ used for the observer design

$$A(\rho) = \begin{bmatrix} 0 & 0 & 0 & a_{14}(\rho) \\ a_{21}(\rho) & a_{22}(\rho) & a_{23}(\rho) & 0 \\ 0 & a_{32}(\rho) & a_{33}(\rho) & a_{34}(\rho) \\ 0 & a_{42}(\rho) & a_{43}(\rho) & a_{44}(\rho) \end{bmatrix}$$

where

$$\begin{aligned}
a_{14}(\rho) &= 1 \\
a_{21}(\rho) &= -9.7851 \\
a_{22}(\rho) &= -0.0061 - 2.1091 \times 10^{-5}\rho_2 - 2.2374 \times 10^{-8}\rho_4 \\
a_{23}(\rho) &= 5.7733 - 84.5625\rho_1 - 0.0351\rho_2 - 0.7450\rho_3 - 7.7365 \times 10^{-5}\rho_4 - 0.0016\rho_5 \\
a_{32}(\rho) &= -5.2124 \times 10^{-4} - 6.2678 \times 10^{-7}\rho_2 + 1.1121 \times 10^{-11}\rho_4 \\
a_{33}(\rho) &= -0.5935 - 0.0026\rho_2 \\
a_{34}(\rho) &= 0.9914 \\
a_{42}(\rho) &= -4.9579 \times 10^{-4} - 3.8893 \times 10^{-6}\rho_2 - 7.6201 \times 10^{-9}\rho_4 + 1.9644 \times 10^{-12}\rho_6 \\
a_{43}(\rho) &= -1.9626 + 3.4170\rho_1 - 0.0173\rho_2 + 0.0301\rho_3 - 3.8081 \times 10^{-5}\rho_4 + 6.63 \times 10^{-5}\rho_6 \\
a_{44}(\rho) &= -0.4609 - 0.0020\rho_2
\end{aligned} \tag{71}$$

$$B(\rho) = \begin{bmatrix} 0 & 0 & 0 \\ 0 & 0 & b_{23}(\rho) \\ b_{31}(\rho) & 0 & b_{33}(\rho) \\ b_{41}(\rho) & b_{42}(\rho) & b_{43}(\rho) \end{bmatrix}$$

where

$$\begin{aligned} b_{23}(\rho) &= 1.3323 \times 10^{-5} - 5.8133 \times 10^{-7}\rho_1 \\ b_{31}(\rho) &= -0.0358 - 1.1877 \times 10^{-5}\rho_2 + 1.5311 \times 10^{-6}\rho_4 + 3.9135 \times 10^{-9}\rho_6 \\ b_{33}(\rho) &= -3.6326 \times 10^{-9} - 5.8732 \times 10^{-8}\rho_1 + 1.6002 \times 10^{-11}\rho_2 + 2.5871 \times 10^{-10}\rho_3 \\ b_{41}(\rho) &= -1.7696 - 0.0089\rho_2 + 5.9851 \times 10^{-5}\rho_4 + 4.4285 \times 10^{-7}\rho_6 + 6.9127 \times 10^{-10}\rho_7 \\ b_{42}(\rho) &= -3.9993 - 0.0352\rho_2 - 7.7600 \times 10^{-5}\rho_4 \\ b_{43}(\rho) &= 1.5328 \times 10^{-7} \end{aligned} \tag{72}$$

VII.B. The linear gains $G_{la}(\rho)$ for actuator fault reconstruction

$$G_{la}(\rho) = \begin{bmatrix} 0 & 0 & g_{la13}(\rho) \\ g_{la21}(\rho) & g_{la22}(\rho) & 0 \\ g_{la31}(\rho) & g_{la32}(\rho) & g_{la33}(\rho) \\ g_{la41}(\rho) & g_{la42}(\rho) & g_{la43}(\rho) \end{bmatrix}$$

where

$$\begin{aligned} g_{la13}(\rho) &= 1 \\ g_{la21}(\rho) &= 1.4939 - 2.1091 \times 10^{-5}\rho_2 - 2.2374 \times 10^{-8}\rho_4 \\ g_{la22}(\rho) &= 5.7733 - 84.5625\rho_1 - 0.0351\rho_2 - 0.7450\rho_3 - 7.7365 \times 10^{-5}\rho_4 - 0.0016\rho_5 \\ g_{la31}(\rho) &= -5.2124 \times 10^{-4} - 6.2678 \times 10^{-7}\rho_2 + 1.1121 \times 10^{-11}\rho_4 \\ g_{la32}(\rho) &= -0.5935 - 0.0026\rho_2 \\ g_{la33}(\rho) &= 0.9914 \\ g_{la41}(\rho) &= -4.9579 \times 10^{-4} - 3.8893 \times 10^{-6}\rho_2 - 7.6201 \times 10^{-9}\rho_4 + 1.9644 \times 10^{-12}\rho_6 \\ g_{la42}(\rho) &= -1.9626 + 3.4170\rho_1 - 0.0173\rho_2 + 0.0301\rho_3 - 3.8081 \times 10^{-5}\rho_4 + 6.63 \times 10^{-5}\rho_6 \\ g_{la43}(\rho) &= -0.4609 - 0.0020\rho_2 \end{aligned} \tag{73}$$

VII.C. The linear gains $G_{la_{aug}}(\rho)$ for sensor fault reconstruction

$$G_{la_{aug}}(\rho) = \begin{bmatrix} g_{la_{aug}11}(\rho) & g_{la_{aug}12}(\rho) & g_{la_{aug}13}(\rho) & 0 \\ g_{la_{aug}21}(\rho) & g_{la_{aug}22}(\rho) & g_{la_{aug}23}(\rho) & 0 \\ g_{la_{aug}31}(\rho) & 0 & g_{la_{aug}33}(\rho) & 0 \\ 0 & g_{la_{aug}42}(\rho) & 0 & 0 \\ 0 & 0 & g_{la_{aug}53}(\rho) & g_{la_{aug}54}(\rho) \end{bmatrix}$$

where

$$\begin{aligned} g_{la_{aug}11}(\rho) &= -0.5935 - 0.0026\rho_2 \\ g_{la_{aug}12}(\rho) &= 0.9914 \end{aligned}$$

$$
\begin{aligned}
g_{la_{aug}13}(\rho) &= -5.2124 \times 10^{-4} - 6.2678 \times 10^{-7}\rho_2 + 1.1121 \times 10^{-11}\rho_4 \\
g_{la_{aug}21}(\rho) &= -1.9626 + 3.4170\rho_1 - 0.0173\rho_2 + 0.0301\rho_3 - 3.8081 \times 10^{-5}\rho_4 + 6.63 \times 10^{-5}\rho_6 \\
g_{la_{aug}22}(\rho) &= -0.4609 - 0.0020\rho_2 \\
g_{la_{aug}23}(\rho) &= -4.9579 \times 10^{-4} - 3.8893 \times 10^{-6}\rho_2 - 7.6201 \times 10^{-9}\rho_4 + 1.9644 \times 10^{-12}\rho_6 \\
g_{la_{aug}31}(\rho) &= 5.7733 - 84.5625\rho_1 - 0.0351\rho_2 - 0.7450\rho_3 - 7.7365 \times 10^{-5}\rho_4 - 0.0016\rho_5 \\
g_{la_{aug}33}(\rho) &= 1.4939 - 2.1091 \times 10^{-5}\rho_2 - 2.2374 \times 10^{-8}\rho_4 \\
g_{la_{aug}42}(\rho) &= 1 \\
g_{la_{aug}53}(\rho) &= -0.1533 \\
g_{la_{aug}54}(\rho) &= -1
\end{aligned}
\tag{74}
$$